Journal of Medicinal Chemistry

Article

pubs.acs.org/jmc

Macromolecular Prodrug That Provides the Irinotecan (CPT-11) Active-Metabolite SN-38 with Ultralong Half-Life, Low C_{max}, and Low Glucuronide Formation

Daniel V. Santi,* Eric L. Schneider, and Gary W. Ashley

ProLynx, 455 Mission Bay Boulevard South, Suite 145, San Francisco, California 94158, United States

Supporting Information

ABSTRACT: We have recently reported a chemical approach for half-life extension that utilizes β-eliminative linkers to attach amine-containing drugs or prodrugs to macromolecules. The linkers release free drug or prodrug over periods ranging from a few hours to over 1 year. We adapted these linkers for use with phenol-containing drugs. Here, we prepared PEG conjugates of the irinotecan (CPT-11) active metabolite SN-38 via a phenyl ether that release the drug with predictable long half-lives. Pharmacokinetic studies in the rat indicate that, in contrast to other SN-38 prodrugs, the slowly released SN-38 shows a very low C_{max}, is kept above target concentrations for extended periods, and forms very little SN-38 glucuronide (the precursor of enterotoxic SN-38). The low SN-38 glucuronide is attributed to low hepatic uptake of SN-38. These macromolecular prodrugs have unique pharmacokinetic profiles that may translate to less intestinal toxicity and interpatient variability than the SN-38 prodrugs thus far studied.

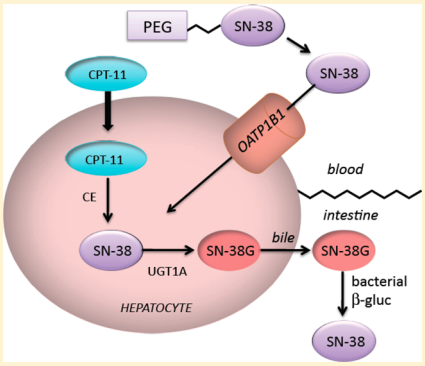

INTRODUCTION

Conjugation of drugs to macromolecular carriers is an established strategy for improving pharmacokinetics. In one approach, the drug is covalently attached to a long-lived circulating macromolecule, such as poly(ethylene glycol) (PEG), through a linker that is slowly cleaved to release the native drug.[1,2] Most of these conjugates use ester-containing linkers that cleave either by spontaneous or esterase-catalyzed reactions and have several limitations: (a) the rate of cleavage can be faster, but not slower than the spontaneous hydrolytic rate, and PEG–ester conjugates have half-lives of about 12–30 h at pH 7.4,[1−5] (b) they can show intra- and interspecies variability of in vivo cleavage rates because of different esterase levels, and (c) cleavage rates are not generally predictable or easily adjustable.

We have recently reported conjugation linkers that self-cleave by a nonenzymatic β-elimination reaction in a highly predictable manner and with a large range of half-lives of cleavage spanning hours to over a year at physiological pH.[6] In this approach, a macromolecular carrier is attached to a linker that is attached to a drug via a carbamate group (**1**; Scheme 1); the β-carbon has an acidic carbon–hydrogen bond (C–H) and also contains an electron-withdrawing modulator (Mod) that controls the pK_a of that C–H bond. Upon hydroxide-ion-catalyzed proton removal (**2**), a rapid β-elimination occurs to cleave the linker–carbamate bond and to release the free drug or prodrug and a substituted alkene **3**. The rate of drug release is proportional to the acidity of the proton, which is controlled by the chemical nature of the modulator; thus, the rate of drug release is controlled by the modulator. It was shown that both in vitro and in vivo cleavages were linearly correlated with electron-withdrawing effects of the modulators and, unlike ester bonds commonly used in releasable linkers,[2] the β-elimination reaction was not catalyzed by general bases or serum enzymes. With releasable conjugates of this type, the terminal half-life ($t_{1/2,\beta}$) of a rapidly cleared released drug is transformed into that of the conjugate and has a longer $t_{1/2,\beta}$ and diminished C_{max} compared to repeated bolus doses of a short-lived drug.

Recently, we described an approach to adapt such β-eliminative linkers for use with phenol-containing drugs (Scheme 2, **4**).[7] In addition to the pK_a modulator, the modified linkers include a methylene adaptor that connects the carbamate nitrogen to the oxygen atom of the drug and an electron-withdrawing *N*-aryl stabilizer that inhibits undesirable cleavage of the adaptor–oxygen bond. Upon β-elimination (Scheme 2, path A), a carbamic acid is released, which rapidly disassembles to the free phenol-containing drug. Spontaneous S_N1 and acid-catalyzed solvolytic reactions were also characterized (Scheme 2, paths B and C); here, an iminium ion of the carbamate (**9**) is formed to assist prodrug expulsion that ultimately loses formaldehyde to give an *N*-aryl carbamate.

We were interested in applying this technology to produce conjugates of SN-38 with very long half-lives. SN-38 is the active metabolite of the anticancer agent irinotecan (CPT-11), primarily used to treat colon cancer, and is one of the most potent known inhibitors of topoisomerase 1 (topo 1). CPT-11 is extensively metabolized and shows large interpatient variability in its pharmacokinetics, pharmacodynamics, and toxicities;[8] it can be reasoned that direct administration of SN-

Received: October 23, 2013
Published: February 4, 2014

   dx.doi.org/10.1021/jm401644v | J. Med. Chem. 2014, 57, 2303−2314

Scheme 1

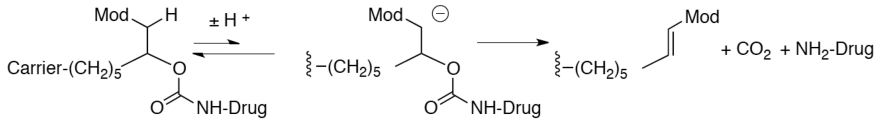

1 2 3

38 might escape some of the metabolism of CPT-11 and thus reduce some of the variability. However, SN-38 is too insoluble to administer directly and has a short half-life and thus requires the use of soluble prodrug depots, such as CPT-11 or conjugates of long-lived macromolecules.

SN-38 prodrugs are usually administered as an i.v. bolus every 1 or 3 weeks. However, topo 1 inhibitors such as SN-38 display time-dependent cytotoxicity because prolonged exposure is needed to inhibit topo 1 during DNA replication. Hence, continuous, protracted administration of low-dose topo 1 inhibitors may be advantageous over the commonly used intensive bolus delivery. It has been proposed that a minimum threshold of exposure to a topo 1 inhibitor (i.e., continuous inhibition) must be achieved for optimal antitumor activity and that a higher dose intensity enhances toxicity but not tumor regression.[9−11] To improve delivery of SN-38, numerous PEG conjugates of CPT-11 or SN-38 with cleavable ester-containing linkers have been developed.[12] Although these are somewhat longer acting than CPT-11, they still achieve a time-over-target concentration for only a small fraction of the dosing schedules used. Indeed, none of the current conjugates maintains the concentration of free SN-38 over the target threshold for protracted periods, nor are they able to because, unless somehow protected, they are limited by the relatively short half-lives of 12 to 30 h for hydrolysis of ester linkages.[1−4] In addition, all of the current SN-38 prodrugs show high C_{max} values of SN-38 that likely contribute to toxicities.

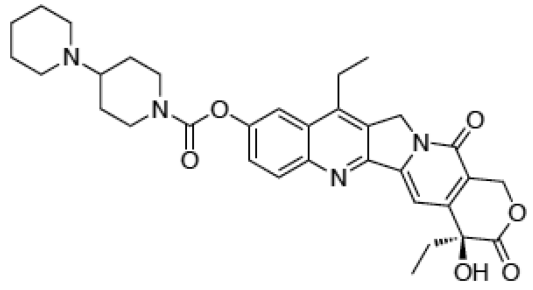

Irinotecan (CPT-11)

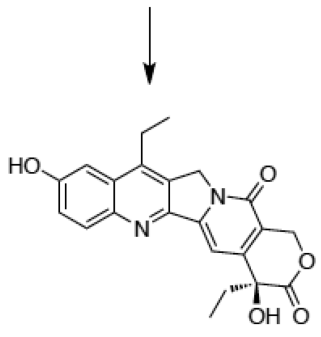

SN-38

Scheme 2

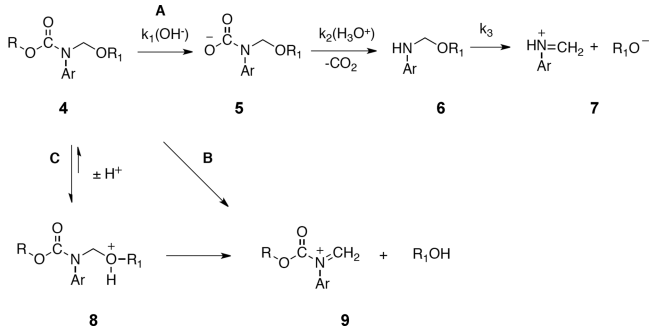

In the present work, we describe the synthesis, properties, and pharmacokinetics of a series of PEG−SN-38 conjugates that use β-eliminative linkers to connect PEG to the 10-phenolic group of SN-38 via a stable ether linkage. Using appropriate pK_a modulators, the in vitro and in vivo half-life of drug release can be controlled from several to ∼400 h, and conjugates were obtained that achieve time-over-threshold concentrations of SN-38 for long periods of time with low C_{max} and very low SN-38 glucuronide (SN-38G) formation. Taken together, these features suggest that the conjugates described here may show high efficacy with lower toxicity and interpatient variability.

RESULTS

Synthesis. On the basis of procedures described for conjugation of phenols to β-eliminative linkers,[7] we prepared PEG−SN-38 conjugates **14A−E** and **16D,E** (Scheme 3). For the carbamate stabilizer, we used 4-NH_2PhCON$(Et)_2$ (pK_a 3.5) because of its suppression of S_N1 solvolysis of analogous compounds[7] and its relationship to amides of *p*-aminobenzoic acid that are generally safe. Azidoalcohols **10A−E** were converted to *N*-aryl carbamates **11A−E** via chloroformate reaction with 4-NH_2PhCON$(Et)_2$. The carbamates were treated with TMSCl/paraformaldehyde to provide the reactive *N*-chloromethyl carbamates **12A−E**. Reaction of **12A−E** with the SN-38 10-oxyanion (10-OH, pK_a 8.56[13]) gave the corresponding C-10 ethers **13A−E**, which were connected to 4-arm PEG_{40kDa}-$(DBCO)_4$ by Cu-free click chemistry to form PEG conjugates **14A−E** in near quantitative yield.[14] To synthesize a less hydrophobic conjugate that was more economical to prepare, we developed a method to attach the linker to PEG via an amide bond. Here, azido linker−SN-38 **13D,E** were reduced with Me_3P to the corresponding amine linker−SN-38 analogues **15D,E**, which were reacted with 4-arm PEG_{40kDa}−*N*-hydroxysuccinimido ester to give **16D,E**.

Solvolysis Products of *N*-Aryl-*N*-SN-38−CH_2-carbamates. The solvolysis products of *N*-aryl-*N*-SN-38−CH_2-carbamates **13** and **14** identify the pathways of SN-38 release. β-Eliminative cleavage (Scheme 2, path A) should give SN-38, the aryl amine, and an alkene (ModCH=CHR), whereas

dx.doi.org/10.1021/jm401644v | J. Med. Chem. 2014, 57, 2303−2314

Scheme 3

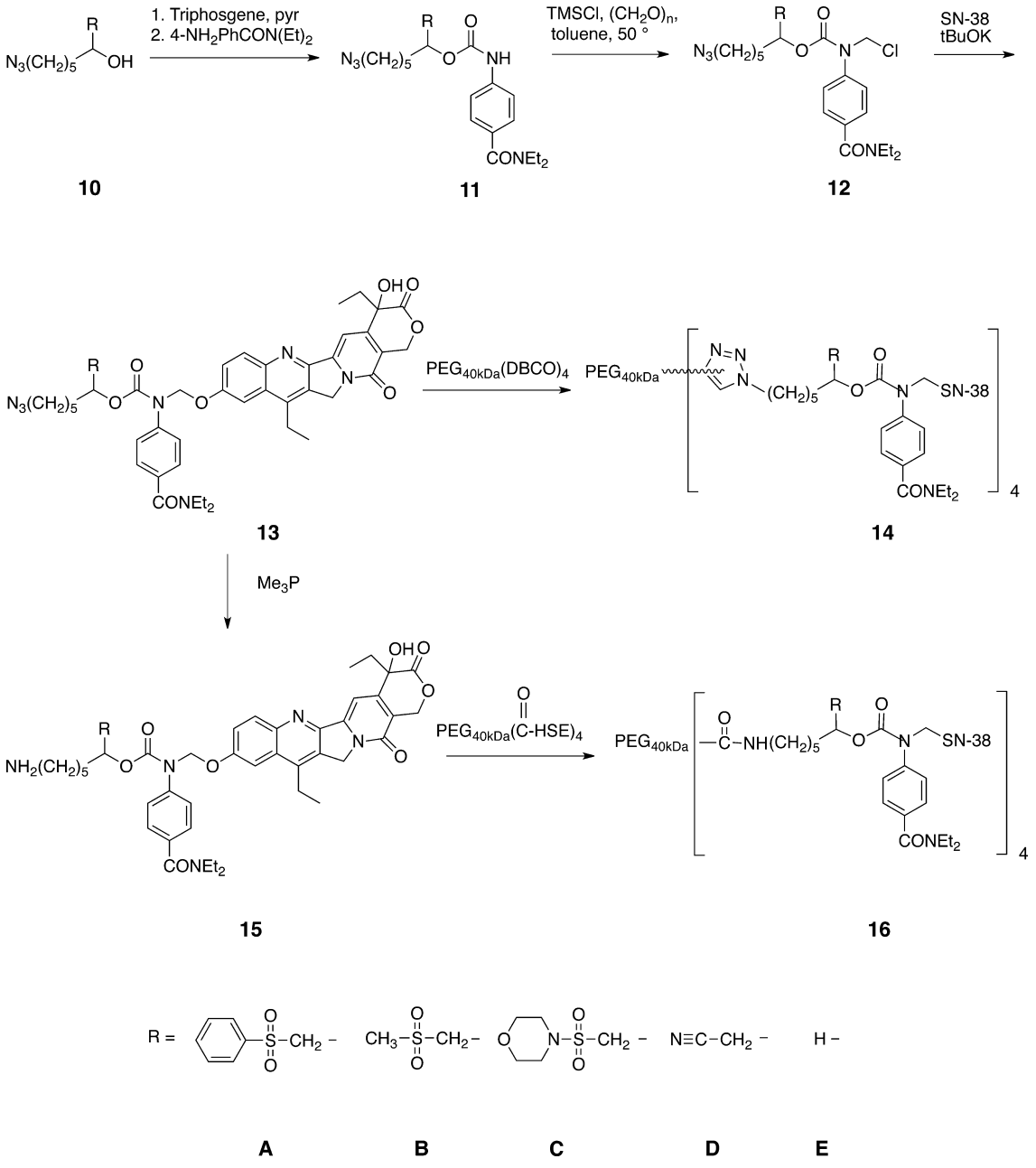

spontaneous (path B) or acid-catalyzed (path C) reactions should both provide SN-38 and *N*-aryl carbamate **11**.[7] Over most of the pH range studied, the insolubility of the SN-38 product required use of such low concentrations (≤10 μM) that aryl amine could not be detected by HPLC−UV. However, SN-38 is ionized at low and high pH (pK_a 1.4 and 8.6[13]) and is significantly more soluble. At pH 0, the azido linker−carbamate **13C** (~40 μM) disappeared with concomitant production of SN-38 ($t_{1/2}$ ~ 12 min); an intermediate presumed to be *N*-$HOCH_2$−**11C** initially appeared that converted to final product **11C**. The analogous PEG−SN-38 conjugate **14C** released the expected SN-38, leaving the aryl amine coupled to PEG as the acid-stable *N*-aryl carbamate. At pH 10.5, the azide linker−carbamate **13C** produced stoichiometric quantities of SN-38 and 4-NH_2PhCON(Et)$_2$ at the same rate ($t_{1/2}$ ~ 6 min). Stable analogue **13E** produced SN-38 and carbamate **11E** in acid or basic media.

In Vitro Kinetics of SN-38 Release. The kinetics for solvolysis of the SN-38-containing carbamate without a pK_a modulator (**14E**), described by eq 1, shows an acid-catalyzed rate between pH 0 and 5.5 with a slope of −1.0 in a log k_{obsd} versus pH plot; at higher pH, the rate was pH-independent up to at least pH 9.4. Determinations of spontaneous rates were limited by difficulties of measuring the extremely slow reaction. Conjugates containing pK_a modulators (**14A−D** and **16D**) show an additional hydroxide-catalyzed rate, as in eq 2.

$$k_{obs} = k_{H^+}[H_3O^+] + k_{H_2O} \quad (1)$$

$$k_{obs} = k_{H^+}[H_3O^+] + k_{H_2O} + k_{OH^-}[OH^-] \quad (2)$$

Solvolysis of **14A−D** possessing pK_a modulators were likewise first order in hydronium ion between pH 0 to ~4.5 (Figure 1 and Table 1) and first order in hydroxide ion at pH

dx.doi.org/10.1021/jm401644v | J. Med. Chem. 2014, 57, 2303−2314

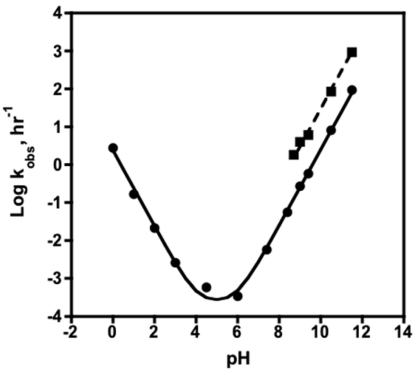

Figure 1. pH–log k_{obsd} profile for solvolysis of **14A**,**C**. For **14A** (––■––), the slope is +1.0 (r^2 = 0.993) between pH 8.7 and 11.5. The solvolysis of **14C** (—●—) was fit to eq 2 from pH 0 to 11.5 using the k_{H_2O} rate of **14E**; the slope from pH 0 to 4 is −1.0 (r^2 = 0.989) and from 6 to 11.5 is +1.0 (r^2 = 0.999).

≥6. The rate of S_N1 solvolysis of **14C**, as estimated by the S_N1 reaction of **14E**, was in agreement with the nadir of the pH–log k_{obsd}. Also, the S_N1 reaction of **14E** was ∼7-fold slower than the corresponding *p*-nitrophenyl ether, which is in accord with the finding that rates of such reactions are inversely related to the pK_a of the leaving group.[15] Of primary relevance are the base-catalyzed rates dictated by the pK_a modulators and the difference between these rates and the spontaneous solvolysis rate at physiological pH. The acid-catalyzed rates, which are independent of the pK_a modulator, primarily provide guidance in handling of samples in pharmacokinetic studies to prevent ex vivo hydrolysis and to assist design of long-term storage conditions.

Table 1 shows that the rates of base-catalyzed *β*-elimination are directly related to the electron-withdrawing ability of the modulator, and at pH 7.4, they have half-lives ranging from ∼9 to 450 h. The rate of **14A** is only slightly slower than that of the analogous *p*-nitrophenyl ether, indicating little dependence of the *β*-elimination reaction on the leaving group pK_a of the ether.[7] They are, however, 6- to 8-fold faster than reported simple primary carbamates with the same modulators[6] because of the higher acidity of the initially formed carbamic acids.[7] Importantly, *β*-elimination rates dominate the significantly slower spontaneous S_N1 hydrolysis at physiological pH. It is noteworthy that for **14D** and **16D** the solvolysis rates are relatively unaffected by the spatially remote DBCO or amide connectors to the PEG macromolecule.

Mechanism. The pH-independent spontaneous hydrolysis of **14E** has precedence in the analogous reactions of N-substituted *N*-aryloxy-[7,15] and *N*-acyloxy-methyl[16] carbamates. There is a spontaneous release of the leaving group with assistance of an iminium ion intermediate (Scheme 2, path B).

The acid-catalyzed solvolysis is first order in hydronium ion from pH 0 to ∼4.5, indicating preprotonation of a site with pK_a < 0 prior to cleavage. The quinoline nitrogen of SN-38 has a pK_a of 1.4,[13] but its protonation is not apparent from the pH–log k_{obsd} profile (Figure 1). Thus, the kinetically relevant protonation must occur at a site remote from and unaffected by protonation of quinoline nitrogen. Because it is unlikely that protonation of the ether linkage of **14** would be unaffected by protonation of SN-38, the site of preprotonation may be the carbonyl oxygen, as proposed for analogous aryl ethers.[7]

As with other *β*-eliminative carbamates[6,7] conjugates with a pK_a modulator, **14A**–**D** showed release rates of SN-38 that were first order in hydroxide ion (Table 1). In the absence of an ionizable proton at the *β*-position of the carbamate (i.e., **14E**), SN-38 release was extremely slow and did not exhibit hydroxide-ion catalysis. Thus, as shown for related ethers[7] and depicted in Scheme 2, path A, the base-catalyzed reaction involves *β*-eliminative cleavage of the *O*-alkyl bond of the carbamate to form carbamic acid **5**; subsequently, there is decarboxylation, which, from related models,[17] is acid-catalyzed, followed by spontaneous collapse[18] of the neutral Mannich base **6** to give CH_2O, the aryl amine, and SN-38.

We desired to determine whether the rate of decarboxylation of the carbamic acid **5** ($k_2[H_3O^+]$, Scheme 2) or collapse of the Mannich base intermediate **6** (k_3, Scheme 2) was slow enough to allow accumulation of intermediates at physiologic pH. For this, we used a previously described[7] kinetic approach that allows an estimate of the lower limit of the rate of collapse of these intermediates at pH 7.4. The rationale is that over the pH range where the hydroxide-catalyzed *β*-elimination is slow compared to subsequent rates the pH–log rate profile has a slope of +1. If the hydroxide-catalyzed rate becomes faster than subsequent reactions, then the pH–log rate profile will have a slope of −1 or 0, depending on the new rate-determining step. Thus, the rate at the highest pH where SN-38 release remains first order in hydroxide allows assignment of a lower limit on the rate of reaction of either intermediate at that pH. Because the rate of reaction either remains the same (spontaneous Mannich base collapse[18]) or decreases (acid-catalyzed decarboxylation[17]) at lower pH, this rate also corresponds to a lower limit of the overall rate of SN-38 release at pH 7.4.

Above pH 8.5, we could directly observe formation of the 10-phenolate ion of SN-38 by continuous spectrophotometric assay, which monitors the relevant C–O bond cleavage step. The log k_{obsd} versus pH profile for SN-38 formation from **14A**,**C** show a slope of +1 to at least pH 11.5. Here, $t_{1/2}$ for **14A** was ∼3 s, so neither intermediate **5** or **6** in Scheme 2, path A have a $t_{1/2}$ > 3 s at that or lower pH. Thus, we conclude that

Table 1. Rates of SN-38 Cleavage from PEG–SN-38 Conjugates

	R	$k_{H_3O^+}$, M^{-1} h^{-1}[a]	k_{OH^-}, M^{-1} h^{-1} × 10^{-3}[a]	$t_{1/2}$, h, pH 7.4	$t_{1/2}$, h, in vivo[b]
14E	H-	9.5 ± 3.0	NA	3600[c]	NA
14A	$PhSO_2CH_2$-	1.2 ± 0.5	301 ± 60	9.2	12
14B	$MeSO_2CH_2$-	1.6 ± 0.7	34 ± 4.0	82	99
14C	$O(CH_2CH_2)NSO_2CH_2$-	2.4 ± 0.4	25 ± 3.8	110	138
14D	$NCCH_2$- (DBCO)	1.4 ± 0.6	6.5 ± 0.6	420	342
16D	$NCCH_2$- (amide)	2.2 ± 0.6	6.1 ± 0.1	450	362

[a]Values are from best fits to first-order acid- or base-catalyzed reactions ± SD. [b]From Table 2. [c]Calculated from k_{H_2O} = 0.19 × 10^{-3} h^{-1} at pH 6.0–9.5.

dx.doi.org/10.1021/jm401644v | J. Med. Chem. 2014, 57, 2303–2314

both intermediates decompose rapidly and would not significantly accumulate at pH 7.4.

Pharmacokinetics. For pharmacokinetic studies of releasable PEG conjugates with slow cleavage rates, the longer $t_{1/2}$ of PEG in the rat (ca. 30−40 h) compared to mouse (12−24 h) makes it the preferred rodent model. PEG−SN-38 conjugates **14A−E** and **16D,E** were administered i.v. to rats, blood samples were removed at various times and immediately quenched in acidified citrate to avoid ex vivo linker cleavage, and plasma was obtained by centrifugation; samples were analyzed by HPLC using UV and fluorescence detection.

Pharmacokinetic data for PEG−SN-38 conjugates, SN-38, and SN-38G in the rat were fit to a two-compartment model depicted in Figure 2 (see Supporting Information for derivations); relevant data with selected values normalized to constant PEG−SN-38 concentrations are summarized in Table 2, and all original data is provided in the Supporting Information. In a separate experiment, C_{max} and AUC were linear over a range of at least 1 to 4 μmol of **16D**. For comparison, reported pharmacokinetic parameters after a 60 mg kg^{-1} bolus dose of CPT-11 in rats that gave a SN-38 C_{max} similar to that from **16D** (0.38 nM) were $C_{max,CPT-11}$ 47 nM and $t_{1/2,CPT-11}$ 2.8 h, $C_{max,SN-38}$ 0.43 nM and $t_{1/2,SN-38}$ 8 h, $C_{max,SN-38G}$ 0.81 nM and $t_{1/2,SN-38G}$, 9.2 h, and AUC_{SN-38G}/AUC_{SN-38} 5.5.[19]

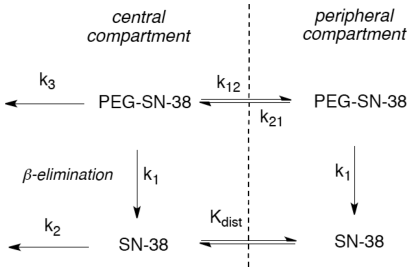

Figure 2. Two-compartment model for releasable PEG−SN-38 conjugates and released SN-38. Rate constant k_1 is for SN-38 release from the conjugate, k_2 and k_3 are for elimination of the SN-38 and intact conjugate, respectively, from the central compartment, and k_{12} and k_{21} are for distribution of the conjugate between the central and peripheral compartments; K_{dist} describes partitioning of the free drug between central and peripheral compartments. Derivations are given in the Supporting Information.

Preliminary pharmacokinetic experiments of **16D**, **16E**, and CPT-11 were also performed in the African green monkey. Overall, the AUC of SN-38 derived from CPT-11 over the first 4 h was only ∼2% of CPT-11, but SN-38G was formed in large amounts such that $AUC_{SN-38G}/AUC_{CPT-11}$ was 0.32 and AUC_{SN-38G}/AUC_{SN-38} was 15. In view of the high SN-38 + SN-38G derived from CPT-11 (33%), it is likely that, as suggested for the rhesus monkey,[20] the low levels of SN-38 are a consequence of high glucuronidation rather than decreased production. In striking contrast, **16D** gave similar SN-38 levels as in rats and a very low AUC_{SN-38G}/AUC_{SN-38} of 0.23. Interestingly, the linker cleavage $t_{1/2}$ in the monkey (360 h) was almost identical to that in the rat (362 h), indicating that the SAR of in vitro versus in vivo cleavage[6] likely holds in animals other than rodents.

Finally, we saw no free SN-38 in plasma of rats or monkeys treated with stable conjugates **14E** and **16E** that cannot undergo β-eliminative release; because we can detect SN-38 at levels <0.1% of conjugate (e.g., **16D**, Table 2), we conclude that there is no significant carbamate hydrolysis that might arise from the action of some unidentified protease or esterase.

We have shown[6] that the steady-state rate for loss of a cleavable conjugate is $k_\beta = k_1 + k_3$, where k_1 is the rate constant for β-elimination and k_3 is the renal elimination rate of the conjugate. The k_3 values were estimated for the DBCO- and amide-linked conjugates using the elimination rate of the corresponding stable conjugates, **14E** or **16E**, as surrogates that can only undergo clearance. Examples of the method to determine in vivo cleavage rates, k_1, are given in Figure 3A,B, with complete data for all conjugates presented in Table 2. Figure 3C,D shows the C versus t profiles of PEG−SN-38 conjugates, SN-38, and SN-38G with the highest and lowest k_1 values, respectively. As shown, the PEG−SN-38 conjugates give very low levels of SN-38G, with AUC_{SN-38G}/AUC_{SN-38} ratios ranging from only 0.08 to 0.2, and the ratios track the rate of linker cleavage, k_1.

DISCUSSION

Rationale for Slow-Releasing PEG−SN-38 Conjugates. Topo 1 inhibitors, such as SN-38, bind and stabilize the enzyme−DNA covalent complex to prevent DNA religation during S phase and thus cause time-dependent DNA damage and apoptosis. Because binding is reversible, constant exposure to the inhibitor is needed to maintain the complex until irreversible events occur that lead to cell death.[21,22] Inhibitors of topo 1 also show a time-dependent increase of in vitro cytotoxicity.[23,24]

Preclinical and clinical studies have also suggested that low-dose, prolonged exposure of topo 1 to inhibitors may be less toxic and more efficacious than conventional high-intensity treatments. It has been convincingly demonstrated that continuous infusion of CPT-11 over 4 days is significantly less toxic than equivalent four daily bolus doses.[19] Houghton et al.[9−11] showed that the efficacy of CPT-11 in human tumor xenografts and in humans is highly schedule-dependent: a given dose administered on a protracted schedule over 21 days was more efficacious than dose-intensive schedules. They proposed that a minimum threshold of the drug must be maintained over long periods for optimal antitumor activity; higher dose-intensity did not provide further benefit, but it enhanced toxicity. Several phase 1 clinical trials of low-dose continuous infusions, including 1 to over 9 weeks of CPT-11, yielded steady-state levels of SN-38 of ∼3 to 15 nM, confirming the tolerability and feasibility of low, protracted dosing.[25−28] Similar phase 1 trials of continuous infusions of the topo 1 inhibitor topotecan also showed activity in several tumors,[29−32] again suggesting that efficacy may be achieved by time-over-target inhibition. Thus, topo 1 inhibitors may display exposure-time-dependent rather than concentration-dependent cytotoxicity: achieving a high inhibitor concentration for a short period does not necessarily produce the same effect as maintaining a low concentration for a prolonged period, even if the total AUC per treatment period are equal.

Although promising, none of the phase 1 trials of protracted continuous infusion of topo 1 inhibitors have been taken forward in adequately powered clinical trials; a major impediment is the impractical requirement for continuous infusions to a large number of patients. A possible solution to this problem is to use long-lived macromolecular drug conjugates that slowly release the drug at low levels over long periods. Toward that end, numerous macromolecular conjugates of CPT analogues have been prepared and stud-

dx.doi.org/10.1021/jm401644v | J. Med. Chem. 2014, 57, 2303−2314

Table 2. Pharmacokinetic Parameters for PEG−SN-38 Conjugates 14 and 16, Released SN-38 and SN-38G in the Rat

conjugate	14E	16E	14A	14B	14C	14D	16D
R-	H-	H-	$PhSO_2CH_2$-	$MeSO_2CH_2$-	$O(CH_2)_2NSO_2CH_2$-	$NCCH_2$-	$NCCH_2$-
PEG connector	DBCO	amide	DBCO	DBCO	DBCO	DBCO	amide
PEG−SN-38							
μmol SN-38	0.22	0.54	2.3	1.0	3.8	3.1	4.9
C_{max}, μM	86	36	379	116	579	387	623
V_d, L kg^{-1}	0.011	0.055	0.025	0.032	0.025	0.029	0.029
$t_{1/2,\beta}$, h	39	58	9	28	30	35	50
$t_{1/2}$ cleavage (ln 2/k_1), h	[a]		12	99	138	342	362
$AUC_{0-\infty}$, μM h	2132	1768	3632	3076	12 440	7588	16 664
N−$AUC_{0-\infty}$, μM h[b]	*47 485*	*16 043*	*7738*	*15 072*	*16 041*	*11 994*	*16 664*
$C_{0,PEG\text{-}SN\text{-}38}$[c]	32	19.6	177	51	247	118	199
N−$C_{0,PEG,SN\text{-}38}$	*713*	*178*	*377*	*250*	*319*	*187*	*199*
SN-38							
C_{max}, μM			1.4		0.18	0.18	0.38
N−C_{max}, μM			*2.98*			*0.28*	*0.38*
$t_{1/2,\beta}$, h			9		34	38	58
$AUC_{0-\infty}$, μM h			13.1		6	4.2	10.9
N−$AUC_{0-\infty}$, μM h			*27.9*		*7.7*	*6.6*	*10.9*
$C_{0,SN\text{-}38}$			1.27		0.154	0.065	0.137
N−$C_{0,SN\text{-}38}$			*2.71*		*0.20*	*0.10*	*0.14*
SN-38G							
C_{max}, μM			0.277		0.019	0.017	0.026
N−C_{max}, μM			*0.590*			*0.027*	*0.026*
$AUC_{0-\infty}$, μM h			2.7		0.83	0.45	0.86
N−$AUC_{0-\infty}$, μM h			*5.75*		*1.07*	*0.71*	*0.86*
Ratios							
$AUC_{SN\text{-}38G}/AUC_{SN\text{-}38}$			0.21		0.14	0.11	0.079

[a]Not applicable or not determined. [b]The prefix N- with an italicized entry designates that values have been normalized to a constant dose of 4.9 μmol of SN-38 content in PEG−SN-38 conjugate **16D**. [c]C_0 is the concentration at t = 0 extrapolated from $t_{1/2,\beta}$.

ied;[12,33,34] in the forefront are three PEGylated conjugates with cleavable ester linkers that have yielded promising results in clinical trials: NKTR-102,[35,36] a PEGylated CPT-11 with a Gly-ester linkage to the C-20 alcohol, ENZ-2208, an analogous PEGylated SN-38,[3,37,38] and NK-012, a soluble PEG−Glu_n micelle linked via a Glu ester to the 10-phenol of SN-38.[4,39] The presumed advantages of these macromolecular conjugates are that they provide a slow-release depot of the attached drug and they also accumulate in tumors by the enhanced permeability and retention (EPR) effect[4,37,40] to give rise to high intratumoral concentrations of the released drug.

However, these conjugates all use an ester linkage to attach the drug to the carrier and probably involve serum esterase(s) in drug release. Hence, in addition to variations in metabolism and transport, drug exposure may be subject to variability in serum esterases. Moreover, unless there is some form of protection against hydrolysis in vivo, the rate of spontaneous, noncatalyzed ester cleavage places an upper limit on the cleavage $t_{1/2}$ of a conjugate and hence the $t_{1/2}$ of the released drug. At pH 7.4, the in vitro $t_{1/2}$ for cleavage of a Gly-C20 ester, as in Enz-2208 and NKTR-102, is ∼12 h,[3] and for cleavage of the C10-phenyl ester of NK-012, is 20 h.[4] Indeed, pharmacokinetic data for NKTR-102, Enz-2208, and NK-012 in humans show that >99.5% of the conjugates are lost with $t_{1/2}$ of ∼12−30 h.[36,38,39] The extraordinarily long half-lives of SN-38 released from such conjugates sometimes cited[41] likely include or refer to the prolonged terminal disposition phase of very low, perhaps insignificant subnanomolar levels of SN-38.[42]

As an illustrative example, Figure 4 shows the human C versus t plot for free SN-38 and SN-38G released from the PEG$(Glu)_n$−SN-38 conjugate, NK-012, as constructed from reported parameters at a recommended schedule of q3w cycles.[39] Here, the $t_{1/2}$ for SN-38 release is 20 h, and ∼95% of the SN-38 has cleared by ∼4 days; the time over a presumed 5 nM threshold is only a small fraction of the interval between doses. The exposure, or AUC, is dominated by the early release of SN-38, but the drug remains over target for only ∼2 days; thus, much of the exposure is "wasted AUC". Also shown is a C versus t simulation in humans for SN-38 released from a PEG−SN-38 conjugate, **16D**, that uses a β-eliminative linker with a much longer cleavage $t_{1/2}$ of 362 h . By dosing q3wk, SN-38 can be kept above a target threshold of 5 nM (or higher with increased dose) for the duration of treatment with a very low C_{max} and peak-to-trough ratio. Here, unlike the conjugates linked by esters, $t_{1/2}$ is limited by clearance of the PEG−SN-38 conjugate and not the cleavage $t_{1/2}$ of the linker. Importantly, although the estimated AUC of the SN-38 released by this conjugate is similar to that of NK-012, the exposure displays time dependence rather than concentration dependence. On the basis of the above, we undertook the current studies to develop PEG−SN-38 conjugates that would release continuous low levels of SN-38 for protracted periods, mimicking a continuous infusion insofar as possible with a single injection.

Chemistry of PEG−SN-38 Conjugates. In the present work, we used β-eliminative linkers of carbamates adapted for use in conjugates containing an ether linkage. The approaches for synthesis and mechanistic evaluation follow directly from previous studies.[7] Thus, PEG−SN-38 conjugates **14A−E** containing a DBCO-derived triazole connector between the drug and macromolecule were prepared by a four-step

dx.doi.org/10.1021/jm401644v | J. Med. Chem. 2014, 57, 2303−2314

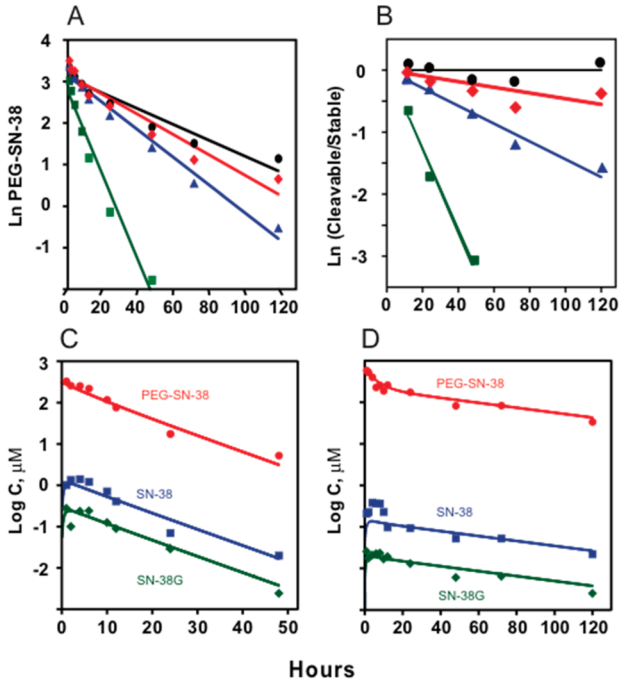

Figure 3. Pharmacokinetic profiles for PEG−SN-38 and SN-38 in the rat. (A) C vs t profile in rat of selected PEG−SN-38 conjugates with different pK_a modulators: **14A** (■, green), **14B** (▲, blue), **14C** (◆, red), and **14E** (●, black). Note that the data is from a different experimental set than reported in Table 2. (B) C vs t plot of ratio of cleavable to stable PEG−SN-38 concentrations vs time. First-order rate constants for linker cleavage (k_1) are obtained as slopes of the lines; for derivation, see the Supporting Information. (C) C vs t plot of PEG−SN-38 conjugate **14A** (●, red), SN-38 (■, blue), and SN-38G (◆, green). (D) C vs t plot of PEG−SN-38 conjugate **16D** (●, red), SN-38 (■, blue), and SN-38G (◆, green).

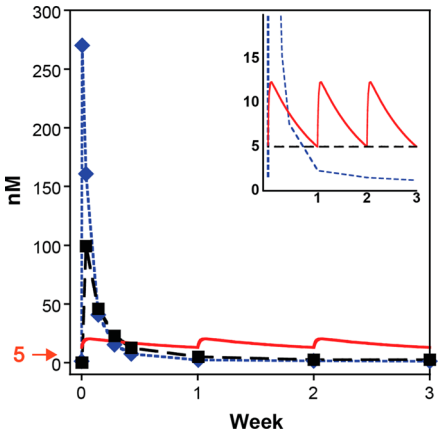

Figure 4. C vs t curves in humans reported for SN-38 and SN-38G derived from NK-012 and from simulations of **16D**. SN-38 (--◆--, blue) and SN-38G (−−■−−, black) in patient plasma after 28 mg m^{-2} q3wk SN-38 equivalents of NK-012; cleavage $t_{1/2}$ 20 h, AUC$_{SN-38}$ 5.4 μM h, and AUC$_{SN-38G}$ 4.1 μM h from Figure 2A in ref 39. SN-38 (—, red) from simulation of PEG−SN-38 conjugate **16D** with −CN pK_a modulator having cleavage $t_{1/2}$ of 362 h after 33 mg m^{-2} qwk × 3 SN-38 equivalents targeting C_{min} 5 nM; inset shows expanded C vs t plot of target 5 nM C_{min} (−−−) and released SN-38 (—, red). Parameters used for simulation were SN-38 V_{SS} 100 L, $t_{1/2}$ 2 h; PEG conjugate $t_{1/2,\beta}$ 168 h. AUC$_{SN-38}$ is 1.4 μM h per injection or 4.3 μM h for 3 weeks.

sequence used for analogous ethers of *p*-nitrophenol (Scheme 3). Conjugates **16D,E** containing a less hydrophobic amide connector were prepared by diverting intermediates **13D,E** to prepare amines **15D,E** used for acylation with a 4-armed PEG$_{40\ kDa}$-HSE.

Solvolysis of conjugates with stable linkers (**14E**, **16E**) at all pH values and those containing modulators (**14A−D** and **16D**) in acidic media gave SN-38 and the *N*-aryl carbamate as final products, indicating initial cleavage of the methylene adaptor−oxygen bond. In contrast, solvolysis of the conjugate containing pK_a modulators at pH > 6 yielded SN-38, the PEG-alkenylsulfone, and 4-(Et)$_2$NCOPhNH$_2$ as products, indicating initial β-eliminative *O*-alkyl cleavage of the carbamate bond.

Kinetic studies of solvolysis of PEG−SN-38 conjugates showed spontaneous, hydronium-ion-, and hydroxide-ion-catalyzed reactions. The acid-catalyzed reaction involves pre-equilibrium protonation of the reactant followed by rate-determining cleavage to SN-38 and the unstable carbamate iminium ion (Scheme 2); the latter would rapidly hydrate to the *N*-hydroxymethyl carbamate and lose formaldehyde in acidic media. Because of several kinetically equivalent mechanisms, it was impossible to assign the exact site of initial protonation from the available data. The precise contribution of the uncatalyzed S$_N$1 pathway cannot be ascertained with linkers containing a pK_a modulator because of competing, more rapid hydroxide-catalyzed β-elimination, but it could be estimated from the nadir of the pH rate profile and the spontaneous solvolysis of stable carbamate **16E**. In the present case, the $t_{1/2}$ of S$_N$1 solvolysis of **16E**, and hence **14A−D** and **16D**, at pH 7.4 is estimated to be ∼3600 h.

The specific base-catalyzed β-eliminative cleavage is driven by the electron-withdrawing effect of the pK_a modulator on the adjacent C−H bond. Depending on the modulator used, the $t_{1/2}$ values at pH 7.4 ranged from ∼10 to 450 h, all significantly faster than the ∼3600 h $t_{1/2}$ for S$_N$1 cleavage. The initial step is the cleavage of the *O*-alkyl bond of the carbamate to give a carbamic acid, which undergoes decarboxylation to the Mannich base[17] and subsequent collapse to the aryl amine, formaldehyde, and free drug (Scheme 2, path A). Using a kinetic approach previously described,[7] we could estimate that at pH 7.4 decarboxylation of carbamic acid **8** and collapse of the Mannich base **9** both occur with $t_{1/2}$ < 3 s at physiologic pH and hence would not accumulate to any significant extent in vivo.

Pharmacokinetic Studies. Accurate determination of SN-38 blood levels in the presence of high levels of cleavable PEG−SN-38 conjugates is challenging. In addition to the high sensitivity needed for SN-38 and SN-38G analysis, precautions are needed to minimize ex vivo cleavage of the relatively high amount of PEG−SN-38 present (up to ∼1800:1 in the present work). A low level of linker cleavage of the conjugate at pH 7.4, occurring after only a few minutes, can result in artifactual increases in free SN-38. Thus, drawn blood samples were rapidly quenched with cold, acidified citrate to pH ∼5.5, and plasma samples were never subjected to conditions (e.g., strong acid) shown to catalyze cleavage. PEG−SN-38 and free SN-38 are easily separated from interfering substances on HPLC and quantitated by UV-fluorescence; however, the SN-38G peak co-eluted with an interfering fluorescent substance from plasma that prevented high-sensitivity analysis. Hence, independent measurements of SN-38G were made after acid treatment to convert it to its lactone form that eluted in a region free of interfering substances.

dx.doi.org/10.1021/jm401644v | J. Med. Chem. 2014, 57, 2303−2314

The cost of prolonged release of SN-38 from the conjugates is a decreased efficiency of drug utilization; that is, when $t_{1/2,cleavage} \gg t_{1/2,\beta}$, the efficiency of SN-38 delivery $[k_1/(k_1 + k_3)]$ is limited by the residence time of PEG. For example, **14A** has a relatively high rate of drug release ($t_{1/2}$ 12 h) compared to renal elimination ($t_{1/2}$ 39 h) but delivers ~76% of its SN-38 cargo; in contrast, **16D**, with a very slow cleavage ($t_{1/2}$ 362 h) delivers only 12% of its SN-38 in the rat, whereas the remainder is excreted unchanged. In humans, the $t_{1/2,\beta}$ of **16D** is estimated to be ~7 days (Figure 4), so the efficiency of SN-38 utilization is increased to ~32%. Thus, an appropriate balance must be reached between the duration of action desired and the economics of SN-38 utilization.

Clearly, it would be desirable to use conjugates with the longest circulating residence times possible. In the cleavable PEG−SN-38 conjugates with a −CN pK_a modulator (**14D** and **16D**) and their stable counterparts (**14E** and **16E**), both DBCO and a simple amide were tested as connecting groups to PEG in the rat. Interestingly, although the cleavage rates were the same, conjugates with simple amide connections to PEG (**16D** and **16E**) showed ~50% longer $t_{1/2,\beta}$ values and over 2-fold increased exposure than corresponding conjugates with a hydrophobic DBCO connection (**14D** and **14E**); the $t_{1/2,\beta}$ values are likewise ~50% longer than the 40 h $t_{1/2}$ of the unsubstituted 4-arm PEG carrier.[35] The SN-38 released from amide-linked **16D** also showed ~1.6-fold increase in AUC compared to the DBCO-linked **14D**. It appears that SN-38 increases $t_{1/2,\beta}$ of the conjugates, whereas the concurrent presence of the hydrophobic DBCO remnant decreases it. It is likely that the SN-38 moiety on the conjugate prolongs $t_{1/2,\beta}$ through its high-affinity binding (~99%) to plasma proteins and blood cells.[43] Because the circulating lifetime of conjugates with slow cleavage rates are limited by renal elimination, an extension of the residence time, as in **16D**, makes the conjugate a more efficient source of SN-38 that would require less frequent administration.

Primary objectives of this work were to develop cleavable PEG−SN-38 conjugates that release SN-38 (a) with predictable long half-lives, (b) with low C_{max} values, and (c) that can be kept above a target concentration for topo 1 inhibition for very long periods. In vivo $t_{1/2}$ values for cleavage of PEG−SN-38 conjugates with various pK_a modulators vary from ~12 to 360 h and agree reasonably well with in vitro $t_{1/2}$ values at pH 7.4 (Table 1). Most are considerably longer than the 12−20 h $t_{1/2}$ values reported for PEG−SN-38 conjugates that require ester cleavage. Whereas the $t_{1/2,\beta}$ of SN-38 in the rat is only about ~22 min,[44] the $t_{1/2,\beta}$ of the SN-38 released from the conjugates vary from 8 to 50 h, up to a 135-fold half-life extension. In rodents, the rapid renal elimination of 4-arm PEG_{40kDa} ($t_{1/2}$ ~1 day in mice, 2 days in rat) does not illustrate the full potential of slowly cleaved linkers in humans, where the renal elimination of PEG is much slower ($t_{1/2}$ ~ 5 to 7 days). Because the rate of linker cleavage is species-independent, knowledge of the $t_{1/2}$ of PEG and pharmacokinetics of the drug in species of interest allows cross-species modeling.[6] Thus, we simulated the C versus t for free SN-38 from our lead conjugate **16D** in humans, which was presented in Figure 4. As shown, SN-38 can be kept above a target concentration of 5 nM for at least 1 week with a very low C_{max} and peak-to-trough ratio. Indeed, the C_{max} of SN-38 in the simulation is ~20- to 30-fold lower than reported for NK-012 and Enz-2208, two ester-linked PEG−SN-38 conjugates in clinical trials.[38,39]

It is of interest to compare the plasma SN-38 levels in rats treated with PEG−SN-38 conjugates to those treated with CPT-11. In a study of the toxicity of CPT-11 as a function of dosing schedule, rats were administered a very high 60 mg (102 μmol) CPT-11 kg^{-1} d^{-1} × 4 as daily boluses or as a continuous infusion.[19] Serious acute and delayed-onset diarrhea and myelosuppresion observed in the bolus injection group were alleviated in the continuous infusion group, illustrating the lower toxicity that can be achieved by time- versus dose-dependent exposure. Nevertheless, SN-38 exposure increased from 1.9 μM h in the bolus dosing to 3.0 μM h in the 4 day infusion, whereas C_{max} dropped from 0.43 to 0.15 μM. After normalizing the 20 μmol kg^{-1} dose of **16D** to 5.5 μmol, 3.6-fold lower than in Table 2, the exposure of SN-38 derived from a single dose of the PEG−SN-38 conjugate is estimated to be 3 μM h, whereas C_{max} is 0.17 μM, closely matching parameters of the SN-38 formed during continuous infusion of CPT-11. Conjugate **16D** also showed an AUC_{SN-38G}/AUC_{SN-38} of 0.08, which is dramatically lower than the 3.6 ratio observed in the 4 day infusion of CPT-11. Thus, with exception of the 45-fold lowering of the glucuronidation ratio, the SN-38 released from a single dose of **16D** closely mimics the SN-38 formed in the 4 day CPT-11 continuous infusion.

The current study has implications for issues of toxicity and interpatient variability frequently observed with other SN-38 prodrugs, namely, CPT-11 and esterase-cleavable PEG−SN-38 and CPT-11 conjugates. CPT-11 is the most widely used prodrug of SN-38; its metabolism is well-understood[45] and explains the late-onset severe diarrhea caused by toxicity to intestinal cells. As illustrated in Figure 5A, CPT-11 is converted into SN-38 by hepatic carboxyesterase (CE), which is then metabolized by hepatic UGT1A to its 10-glucuronide, SN-38G. Glucuronidation facilitates biliary excretion, and bacterial β-glucuronidase causes reconversion of SN-38G to SN-38 in the cecum and colon. Unless intestinal UGT1A converts the drug back to the inert SN-38G,[46,47] the SN-38 exerts toxic effects on the intestine. Thus, as a precursor of SN-38, SN-38G is a source of the intestinal toxin, and as an inert product of SN-38 glucuronidation, SN-38G serves as a protection against intestinal toxicity.

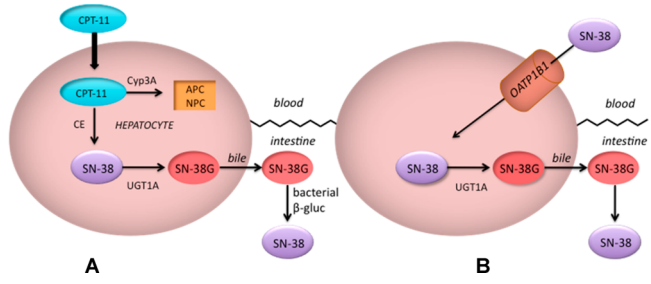

Figure 5. Hepatic uptake of (A) CPT-11 or (B) SN-38 using OATP1B1 transporter and conversion of SN-38 to SN-38G followed by deconjugation by intestinal bacterial β-glucuronidase back to SN-38.

Surprisingly, with the slow-releasing conjugates tested here, plasma SN-38G was barely detectable, with exposure (AUC) representing only ~8% of that of the SN-38 released in our longest-acting conjugate, **16D**. The levels of SN-38G from the other conjugates described here track the linker cleavage rate but are all very low (≤21% of SN-38). In contrast, administration of CPT-11[19,39] by bolus or continuous infusion,

dx.doi.org/10.1021/jm401644v | J. Med. Chem. 2014, 57, 2303−2314

bolus SN-38,[44] or esterase-cleavable PEG−SN-38 or CPT-11 conjugates[36,38,39] results in plasma $AUC_{SN\text{-}38G}/AUC_{SN\text{-}38}$ ratios that can approach 10- to over 100-fold higher than we observe with **16D**. Preliminary results on the pharmacokinetics of **16D** and CPT-11 in the African green monkey track those observed in the rat; that is, the $AUC_{SN\text{-}38G}/AUC_{SN\text{-}38}$ ratio is extremely high for CPT-11 and extremely low for **16D**. Thus, the low SN-38G levels observed for our PEG conjugates in the rat are not due to peculiarities specific to rodents. Although the results may at first seem paradoxical, there is a congruent mechanism that explains the uniquely low SN-38G levels observed here and suggests its relevance to chemotherapy.

In the case of CPT-11, the source of hepatic SN-38 is CE metabolism in the liver; because high blood levels of CPT-11 drive its hepatic uptake, CPT-11 acts as a large and efficient trojan horse for a continuous source of hepatic SN-38. In contrast, as in Figure 5B, SN-38 generated by PEG−SN-38 conjugates in the systemic circulation enters the liver primarily via the organic anion transporter OATP1B1, which does not transport CPT-11 or SN-38G.[48,49] Thus, differential hepatic uptake can explain why CPT-11 results in higher levels of hepatic and plasma SN-38G and hence higher intestinal SN-38 than the very low levels of SN-38 delivered to the liver by the conjugates described here. It appears that the high systemic SN-38G observed after CPT-11 treatment reflects its high hepatic uptake and the detoxification effects of liver and intestinal UGT1A glucuronidation against intestinal exposure to SN-38.[46,47] However, if SN-38G is the source of enterotoxic SN-38, then it is evident that an effective way to avoid the toxic agent is simply to reduce levels of SN-38G in the intestine. Because the low SN-38G formed from analogues described here likely reflects low hepatic uptake of SN-38, it may be surmised that intestinal exposure to SN-38 would likewise be low.

Bolus SN-38[44] or esterase-cleavable PEG−SN-38[38,39] conjugates also produce SN-38G, albeit not at the high levels seen with CPT-11 or the low levels observed with SN-38 conjugates described here; for example, the $AUC_{SN\text{-}38G}/AUC_{SN\text{-}38}$ of NK-012 is ∼1.1 (Figure 4). Because liver SN-38 is associated with intestinal toxicity and blood SN-38, with myelosuppression, it may not be coincidental that the DLT of many PEG−SN-38 prodrugs is neutropenia rather than diarrhea, which can be alleviated by treatment with G-CSF.[38] The long-lived PEG−SN-38 conjugates described here, such as **16D**, show even lower SN-38G than bolus SN-38 or esterase-cleavable PEG−SN-38. This may be explained by the comparatively high C_{max} of free SN-38 that occurs with bolus injection or with the shorter-lived esterase-cleavable conjugates. With these, SN-38 should enter the liver via OATP1B1 in proportion to plasma levels (i.e., C_{max} effect) because SN-38 levels never exceed the ∼20 μM K_m of the transporter.[49]

A prodrug of SN-38 such as **16D** that does not produce significant SN-38G might also result in less interpatient variability than CPT-11 because major sources of variability with CPT-11, namely, CE and Cyp3A, are not involved and UGT1A is not as important. Thus, if the low SN-38G levels formed from long-acting PEG−SN-38 conjugates in the rat translate to humans, then we may achieve therapeutic SN-38 levels without enteric injury and with lower interpatient variability than currently used SN-38 prodrugs.

CONCLUSIONS

We have described the synthesis of PEG−SN-38 conjugates linked by a series of cleavable β-eliminative linkers, their mechanisms of SN-38 release, and their pharmacokinetic properties in rats. Results show that such conjugates provide a unique pharmacokinetic profile to the released SN-38 that differs dramatically from those reported for other SN-38 prodrugs, including CPT-11. First, the presence of SN-38 on the conjugates greatly increases its circulatory residence time, providing a benefit in the duration of action and efficiency of drug delivery. Second, using linkers with very long half-lives for cleavage, SN-38 is delivered with a low C_{max} yet at concentrations that keep the drug over presumed target levels for sustained periods. Third, very low levels of SN-38G are formed, suggesting that toxicities and other pharmacodynamic variabilities seen with other SN-38 prodrugs may be decreased. Last, as well established with other PEG−SN-38 conjugates, we expect accumulation of our conjugates in tumors by the EPR effect[4,37,40] and consequent high intratumoral concentrations of the released drug. We are hopeful that these properties will faithfully translate to humans.

EXPERIMENTAL PROCEDURES

General. Materials purchased were of the purest grade commercially available. HPLC analyses were reverse-phase and used UV or fluorescence detection. Purity of the tested conjugates was all ≥95% as assessed by HPLC, and SN-38/PEG ≥ 3.98. Animal studies were performed at Invitek (rat) and RxGen (monkey). Details are provided in the Supporting Information.

Synthesis. *O-[7-Azido-1-cyano-2-heptyl]-N-[4′-(diethylcarbamoyl)phenyl)]carbamate (11D).* A solution of 7-azido-1-cyano-2-heptanol **10D** (4.6 g, 25.0 mmol) in 200 mL of anhydrous THF was treated with triphosgene (12.5 g, 42.0 mmol) and pyridine (1.6 mL, 50.0 mmol) for 10 min at ambient temperature. The solution was filtered and evaporated to yield the crude chloroformate, which was dissolved in 200 mL of anhydrous THF and treated with 4-(*N*,*N*-diethylcarboxamido)aniline (4.80 g, 25.0 mmol) and triethylamine (7.5 mL, 53.8 mmol) for 1 h. The mixture was diluted with EtOAc and washed successively with water, 1 N HCl, sat. aq. $NaHCO_3$, and brine, dried with $MgSO_4$, filtered, and evaporated. The crude material was chromatographed on SiO_2 using a step gradient of hexane, 1:1 hexane/EtOAc, and 1:2 hexane/EtOAc . The product crystallized on standing and was recrystallized from 1:1 EtOAc/hexane to provide product **11D** (4.4 g, 11.0 mmol, 44%). ^{1}H NMR (400 MHz, $CDCl_3$): δ 7.40 (2H, d, J = 8 Hz; H3′), 7.33 (2H, d, J = 8 Hz; H2′), 7.07 (1H, br s; NH), 4.98 (1H, m; H2), 3.49 (4H, br s; NCH_2), 3.27 (2H, t, J = 6.8 Hz; H7), 2.82 (1H, dd, J = 17, 5.3 Hz; H1a), 2.65 (1H, dd, J = 17, 4.4 Hz; H1b), 1.85 (1H, m; H3a), 1.73 (1H, m; H3b), 1.60 (2H, m; H4), 1.43 (4H, m; H5 + H6), 1.16 (6H, br s; $CH_2\mathbf{CH_3}$). LC−MS m/z: $[M + H]^+$ calcd for $C_{20}H_{29}N_6O_3$, 401.2; found, 401.2.

N-Aryl carbamates **11A−C,E** were prepared in a similar fashion and are described in the Supporting Information.

O-[7-Azido-1-cyano-2-heptyl]-N-(SN-38-CH_2)-N-[4′-(diethylcarbamoyl)phenyl)]carbamate (13D). A mixture of **11D** (400 mg, 1.0 mmol), paraformaldehyde (35 mg, 1.5 mmol), chlorotrimethylsilane (0.5 mL, 4.0 mmol), and 5 mL of anhydrous toluene was heated at 50 °C in a sealed 20 mL vial for 24 h, at which time a clear solution containing a small amount of precipitate was obtained. HPLC analysis of a 5 μL aliquot diluted into 1.0 mL of 4 mM *N*,*N*-diisopropylethylamine in ethanol indicated complete consumption of the starting carbamate (λ_{max} 243 nm) and formation of a slightly later-eluting peak (λ_{max} 231 nm), consistent with the *N*-(ethoxymethyl)-carbamate of **11D**. The solution was cooled to ambient temperature, filtered, and evaporated. The residue was dissolved in 5 mL of dry toluene, filtered, and evaporated to provide 458 mg of an unstable moisture-sensitive yellow oil containing 89% by weight of *N*-(chloromethyl)carbamate **12D** as determined by the HPLC assay. A 1.0 M solution of KO*t*Bu in THF (250 μL, 0.25 mmol) was added to a solution of SN-38 (100 mg, 0.255 mmol) in 10 mL of 1:1 THF/DMF cooled on ice under nitrogen, forming an initial dark green color that changed to a bright gold suspension. After 15 min, a

solution of the crude *N*-(chloromethyl)carbamate (190 mg, 0.36 mmol) in 1 mL of THF was added. After 15 min, the pale yellow solution was diluted with EtOAc, washed sequentially with 5% citric acid, water, and brine, then dried over $MgSO_4$, filtered, and evaporated. Excess DMF was removed by trituration of the oily residue with water, and the residue was dissolved in DCM, dried, and then chromatographed on SiO_2 using a step gradient of hexane, 20, 40, 60, and 80% acetone in hexane, providing purified azido linker−SN-38 **13D** as a pale yellow foam (150 mg, 0.186 mmol, 73%). ^{1}H NMR (400 MHz, $CDCl_3$): δ 8.15 (1H, d, J = 9.2 Hz), 7.60 (1H, s), 7.48 (1H, dd, J = 2, 9 Hz), 7.40 (4H, m), 7.25 (1H, d, J = 2), 5.75 (2H, br), 5.73 (1H, d, J = 16 Hz), 5.28 (1H, d, J = 16 Hz), 5.22 (2H, s), 4.99 (1H, m), 3.84 (1H, s), 3.53 (2H, br), 3.53 (2H, br), 3.17 (2H, t, J = 7 Hz), 3.12 (2H, q, J = 7 Hz), 2.74 (1H, dd, J = 1, 17 Hz), 2.54 (1H, dd, J = 5, 17 Hz), 1.86 (2H, m), 1.6 (1H, m), 1.46 (1H, m), 1.37 (3H, t, J = 7 Hz), 1.25 (6 H, m), 1.12 (4 H, m), 1.02 (3H, t, J = 7.3 Hz). LC−MS m/z: $[M + H]^+$ calcd for $C_{44}H_{51}N_8O_8$, 805.3; found, 805.3.

Compounds **13A−C,E** were prepared in a similar fashion and are described in the Supporting Information. An alternative large-scale preparation of **12D** and **13D** is described in the Supporting Information.

*O-[7-Amino-1-cyano-2-heptyl]-N-(SN-38-CH$_2$)-N-[4′-(diethylcarbamoyl)phenyl)]carbamate Acetate (**15D**).* A 1 M solution of trimethylphosphine in THF (2.9 mL, 2.9 mmol) was added to a solution of **13D** (1.13 g, 1.4 mmol) and acetic acid (0.19 mL, 3.3 mmol) in 10 mL of THF. Gas was slowly evolved. After stirring for 2 h, water (1.0 mL) was added, and the mixture was stirred for an additional 1 h. The residue was partitioned between ether and water. The water phase was washed with EtOAc, and the clear yellow aqueous phase was evaporated to provide 800 mg of yellow foam. This was dissolved in THF, filtered, and quantitated by UV absorbance to provide a solution containing 1.2 μmol (86%) of product. C_{18} HPLC showed a single peak. LC−MS m/z: $[M + H]^+$ calcd for $C_{43}H_{51}N_6O_8$, 779.4; found, 779.3.

Compounds **15A−C,E** were prepared in a similar fashion and are described in the Supporting Information. An alternative large-scale preparation synthetic method of **15D** is described in the Supporting Information.

*O-[7-PEG-triazole-1-cyano-2-heptyl]-N-(SN-38-CH$_2$)]-N-[4′-(diethylcarbamoyl)phenyl)]carbamate (**14D**).* A 30 mM solution of **13D** in THF (400 uL, 12 μmol) was added to a gently stirred solution of 4-arm PEG_{40kDa}-$(DBCO)_4$ (100 mg, 2.5 μmol PEG, 10 μmol DBCO) in 1.0 mL of THF. After 20 h at ambient temperature, the solvent was evaporated, and the residue was dissolved in methanol and dialyzed (SpectraPor 2 membrane, 12 kDa cutoff) against methanol to remove excess azide linker−SN-38. After evaporation of the methanol, the product was taken up in 1 mL of THF and precipitated with 10 mL of MTBE to provide 98 mg of conjugate (2.2 μmol, 88%). Size-exclusion HPLC indicated a single peak corresponding to the conjugate. Complete loss of the DBCO absorbance at 308 nm was noted. Unconjugated SN-38 was 0.6 mol % by reversed-phase HPLC. SN-38 content was determined spectrophotometrically on a 0.45 mg mL^{-1} solution in ACN using $\varepsilon_{363\ nm}$ = 22 500 M^{-1} cm^{-1} to be SN-38/PEG = 3.9. Treatment in basic solution released all SN-38.

PEGylated SN-38 analogues **14A−C,E** were prepared in a similar fashion and are described in the Supporting Information.

*O-[7-PEG-carboxamido-1-cyano-2-heptyl]-N-(SN-38-CH$_2$)]-N-[4′-(diethylcarbamoyl)phenyl)]carbamate (**16D**).* A 50 mM solution of **15D** in ACN (1.2 mL, 60 μmol) was added to a gently stirred solution of 4-arm PEG_{40kDa}-$(NHS)_4$ (500 mg, 12.5 μmol PEG, 50 μmol NHS) in 2.0 mL of ACN followed by addition of *N*,*N*-diisopropylethylamine (20 μL, 150 μmol). After 1 h at ambient temperature, 5 mL of 0.1 M KP_i pH 7.0, was added, and the mixture was dialyzed (SpectraPor 2 membrane, 12 kDa cutoff) sequentially against 50:50 methanol/water and methanol to remove excess azide linker−SN-38. After evaporation of methanol, the product was dissolved in 2 mL of THF and precipitated with 10 mL of MTBE to provide 490 mg of conjugate (10.9 μmol conjugate, 87%). Size-exclusion HPLC indicated a single peak corresponding to the conjugate. Unconjugated SN-38 was determined to be 0.6 mol % by reversed-phase HPLC. SN-38 content was determined spectrophotometrically on a 0.45 mg mL^{-1} solution in ACN using $\varepsilon_{363\ nm}$ = 22 500 M^{-1} cm^{-1} to be SN-38/PEG = 3.9. Treatment in basic solution released all SN-38.

PEGylated SN-38 **16E** was prepared in a similar fashion and is described in the Supporting Information. An alternative large-scale preparation of **16D** is described in the Supporting Information.

Kinetic Studies. Kinetic studies were performed by HPLC or spectrophotometric determination of SN-38 anion at pH > 8.5 as described for analogous *p*-nitrophenyl ethers.[7]

Pharmacokinetics. Pharmacokinetic studies were performed on female Sprague−Dawley rats (n = 3 for each conjugate), assayed by HPLC, and analyzed by a two-compartment model, as detailed in Figure 2 and in the Supporting Information.

■ ASSOCIATED CONTENT

Ⓢ Supporting Information

Detailed synthetic procedures and analytical and spectroscopic data for compounds as well as kinetic and pharmacokinetic methods. This material is available free of charge via the Internet at http://pubs.acs.org.

■ AUTHOR INFORMATION

Corresponding Author

*E-mail: Daniel.V.Santi@prolynxllc.com. Phone: 415 552 5306.

Notes

The authors declare the following competing financial interest(s): D.V.S, G.W.A., and E.L.S. are inventors on patent applications protecting the compounds and technologies disclosed in this article.

■ ACKNOWLEDGMENTS

We thank Philip Smith, Pieter Timmermans, and Joseph Dougherty for their comments on this work.

■ ABBREVIATIONS USED

CPT-11, irinotecan; CPT, camptothecin; DBCO, dibenzoazacyclooctyne; EPR, enhanced retention and permeability; HSE, hydroxysuccimide ester; PEG, poly(ethylene glycol); SN-38G, SN-38 10-glucuronide; SN-38, 7-ethyl-10-hydroxy-camptothecin; topo 1, topoisomerase 1

■ REFERENCES

(1) Greenwald, R. B.; Yang, K.; Zhao, H.; Conover, C. D.; Lee, S.; Filpula, D. Controlled release of proteins from their poly(ethylene glycol) conjugates: Drug delivery systems employing 1,6-elimination. *Bioconjugate Chem.* **2003**, *14*, 395−403.

(2) Filpula, D.; Zhao, H. Releasable PEGylation of proteins with customized linkers. *Adv. Drug Delivery Rev.* **2008**, *60*, 29−49.

(3) Zhao, H.; Rubio, B.; Sapra, P.; Wu, D.; Reddy, P.; Sai, P.; Martinez, A.; Gao, Y.; Lozanguiez, Y.; Longley, C.; Greenberger, L. M.; Horak, I. D. Novel prodrugs of SN38 using multiarm poly(ethylene glycol) linkers. *Bioconjugate Chem.* **2008**, *19*, 849−859.

(4) Koizumi, F.; Kitagawa, M.; Negishi, T.; Onda, T.; Matsumoto, S.; Hamaguchi, T.; Matsumura, Y. Novel SN-38-incorporating polymeric micelles, NK012, eradicate vascular endothelial growth factor-secreting bulky tumors. *Cancer Res.* **2006**, *66*, 10048−10056.

(5) Fox, M. E.; Guillaudeu, S.; Frechet, J. M.; Jerger, K.; Macaraeg, N.; Szoka, F. C. Synthesis and in vivo antitumor efficacy of PEGylated poly(l-lysine) dendrimer-camptothecin conjugates. *Mol. Pharmaceutics* **2009**, *6*, 1562−1572.

(6) Santi, D. V.; Schneider, E. L.; Reid, R.; Robinson, L.; Ashley, G. W. Predictable and tunable half-life extension of therapeutic agents by controlled chemical release from macromolecular conjugates. *Proc. Natl. Acad. Sci. U.S.A.* **2012**, *109*, 6211−6216.

(7) Schneider, E.; Robinson, L.; Reid, R.; Ashley, G. W.; Santi, D. V. β-Eliminative releasable linkers adapted for bio-conjugation of macromolecules to phenols. *Bioconjugate Chem.* **2013**, *24*, 1990−1997.
(8) Mathijssen, R. H.; Verweij, J.; Loos, W. J.; de Bruijn, P.; Nooter, K.; Sparreboom, A. Irinotecan pharmacokinetics-pharmacodynamics: The clinical relevance of prolonged exposure to SN-38. *Br. J. Cancer* **2002**, *87*, 144−150.
(9) Furman, W. L.; Stewart, C. F.; Poquette, C. A.; Pratt, C. B.; Santana, V. M.; Zamboni, W. C.; Bowman, L. C.; Ma, M. K.; Hoffer, F. A.; Meyer, W. H.; Pappo, A. S.; Walter, A. W.; Houghton, P. J. Direct translation of a protracted irinotecan schedule from a xenograft model to a phase I trial in children. *J. Clin. Oncol.* **1999**, *17*, 1815−1824.
(10) Ma, M. K.; Zamboni, W. C.; Radomski, K. M.; Furman, W. L.; Santana, V. M.; Houghton, P. J.; Hanna, S. K.; Smith, A. K.; Stewart, C. F. Pharmacokinetics of irinotecan and its metabolites SN-38 and APC in children with recurrent solid tumors after protracted low-dose irinotecan. *Clin. Cancer Res.* **2000**, *6*, 813−819.
(11) Santana, V. M.; Zamboni, W. C.; Kirstein, M. N.; Tan, M.; Liu, T.; Gajjar, A.; Houghton, P. J.; Stewart, C. F. A pilot study of protracted topotecan dosing using a pharmacokinetically guided dosing approach in children with solid tumors. *Clin. Cancer Res.* **2003**, *9*, 633−640.
(12) Venditto, V. J.; Simanek, E. E. Cancer therapies utilizing the camptothecins: a review of the in vivo literature. *Mol. Pharmaceutics* **2010**, *7*, 307−349.
(13) Fassberg, J.; Stella, V. J. A kinetic and mechanistic study of the hydrolysis of camptothecin and some analogues. *J. Pharm. Sci.* **1992**, *81*, 676−684.
(14) Debets, M. F.; van Berkel, S. S.; Schoffelen, S.; Rutjes, F. P.; van Hest, J. C.; van Delft, F. L. Aza-dibenzocyclooctynes for fast and efficient enzyme PEGylation via copper-free (3 + 2) cycloaddition. *Chem. Commun.* **2010**, *46*, 97−99.
(15) Majumdar, S.; Sloan, K. B. Synthesis, hydrolyses and dermal delivery of N-alkyl-N-alkyloxycarbonylaminomethyl (NANAOCAM) derivatives of phenol, imide and thiol containing drugs. *Bioorg. Med. Chem. Lett.* **2006**, *16*, 3590−3594.
(16) Iley, J.; Moreira, R.; Calheiros, T.; Mendes, E. Acyloxymethyl as a drug protecting group: Part 4. The hydrolysis of tertiary amidomethyl ester prodrugs of carboxylic acid agents. *Pharm. Res.* **1997**, *14*, 1634−1639.
(17) Johnson, S. L.; Morrison, D. L. Kinetics and mechanism of decarboxylation of N-arylcarbamates. Evidence for kinetically important zwitterionic carbamic acid species of short lifetime. *J. Am. Chem. Soc.* **1972**, *94*, 1323−1334.
(18) Bundgaard, H.; Johansen, M. Prodrugs as drug delivery systems. XIX. Bioreversible derivitization of aromatic amines by formation of N-Mannich bases with succinimide. *Int. J. Pharm.* **1981**, *8*, 183−192.
(19) Kurita, A.; Kado, S.; Kaneda, N.; Onoue, M.; Hashimoto, S.; Yokokura, T. Alleviation of side effects induced by irinotecan hydrochloride (CPT-11) in rats by intravenous infusion. *Cancer Chemother. Pharmacol.* **2003**, *52*, 349−360.
(20) Inaba, M.; Ohnishi, Y.; Ishii, H.; Tanioka, Y.; Yoshida, Y.; Sudoh, K.; Hakusui, H.; Mizuno, N.; Ito, K.; Sugiyama, Y. Pharmacokinetics of CPT-11 in rhesus monkeys. *Cancer Chemother. Pharmacol.* **1998**, *41*, 103−108.
(21) Pommier, Y. Topoisomerase I inhibitors: Camptothecins and beyond. *Nat. Rev. Cancer* **2006**, *6*, 789−802.
(22) Tanizawa, A.; Fujimori, A.; Fujimori, Y.; Pommier, Y. Comparison of topoisomerase I inhibition, DNA damage, and cytotoxicity of camptothecin derivatives presently in clinical trials. *J. Natl. Cancer Inst.* **1994**, *86*, 836−842.
(23) Levasseur, L. M.; Slocum, H. K.; Rustum, Y. M.; Greco, W. R. Modeling of the time-dependency of in vitro drug cytotoxicity and resistance. *Cancer Res.* **1998**, *58*, 5749−5761.
(24) Hassan, S. B.; Jonsson, E.; Larsson, R.; Karlsson, M. O. Model for time dependency of cytotoxic effect of CHS 828 in vitro suggests two different mechanisms of action. *J. Pharmacol. Exp. Ther.* **2001**, *299*, 1140−1147.
(25) Herben, V. M.; Schellens, J. H.; Swart, M.; Gruia, G.; Vernillet, L.; Beijnen, J. H.; ten Bokkel Huinink, W. W. Phase I and pharmacokinetic study of irinotecan administered as a low-dose, continuous intravenous infusion over 14 days in patients with malignant solid tumors. *J. Clin. Oncol.* **1999**, *17*, 1897−1905.
(26) Masi, G.; Falcone, A.; Di Paolo, A.; Allegrini, G.; Danesi, R.; Barbara, C.; Cupini, S.; Del Tacca, M. A phase I and pharmacokinetic study of irinotecan given as a 7-day continuous infusion in metastatic colorectal cancer patients pretreated with 5-fluorouracil or raltitrexed. *Clin. Cancer Res.* **2004**, *10*, 1657−1663.
(27) Allegrini, G.; Falcone, A.; Fioravanti, A.; Barletta, M. T.; Orlandi, P.; Loupakis, F.; Cerri, E.; Masi, G.; Di Paolo, A.; Kerbel, R. S.; Danesi, R.; Del Tacca, M.; Bocci, G. A pharmacokinetic and pharmacodynamic study on metronomic irinotecan in metastatic colorectal cancer patients. *Br. J. Cancer* **2008**, *98*, 1312−1319.
(28) Takimoto, C. H.; Morrison, G.; Harold, N.; Quinn, M.; Monahan, B. P.; Band, R. A.; Cottrell, J.; Guemei, A.; Llorens, V.; Hehman, H.; Ismail, A. S.; Flemming, D.; Gosky, D. M.; Hirota, H.; Berger, S. J.; Berger, N. A.; Chen, A. P.; Shapiro, J. D.; Arbuck, S. G.; Wright, J.; Hamilton, J. M.; Allegra, C. J.; Grem, J. L. Phase I and pharmacologic study of irinotecan administered as a 96-h infusion weekly to adult cancer patients. *J. Clin. Oncol.* **2000**, *18*, 659−667.
(29) Hochster, H.; Liebes, L.; Speyer, J.; Sorich, J.; Taubes, B.; Oratz, R.; Wernz, J.; Chachoua, A.; Raphael, B.; Vinci, R. Z.; et al. Phase I trial of low-dose continuous topotecan infusion in patients with cancer: An active and well-tolerated regimen. *J. Clin. Oncol.* **1994**, *12*, 553−559.
(30) Hochster, H.; Wadler, S.; Runowicz, C.; Liebes, L.; Cohen, H.; Wallach, R.; Sorich, J.; Taubes, B.; Speyer, J. Activity and pharmacodynamics of 21-day topotecan infusion in patients with ovarian cancer previously treated with platinum-based chemotherapy. New York Gynecologic Oncology Group. *J. Clin. Oncol.* **1999**, *17*, 2553−2561.
(31) Wiernik, P. H.; Li, H.; Weller, E.; Hochster, H. S.; Horning, S. J.; Nazeer, T.; Gordon, L. I.; Habermann, T. M.; Minniti, C. J.; Shapiro, G. R.; Cassileth, P. A. Activity of topotecan 21-day infusion in patients with previously treated large cell lymphoma: long-term follow-up of an Eastern Cooperative Oncology Group study (E5493). *Leuk. Lymphoma* **2012**, *53*, 1137−1142.
(32) Muggia, F.; Kosloff, R.; Liebes, L.; Hochster, H. Topotecan continuous infusion: CA-125 responses including patients pretreated with other schedules of topotecan. *Oncologist* **2006**, *11*, 529−531.
(33) Duncan, R.; Ringsdorf, H.; Satchi-Fainaro, R. Polymer therapeutics–polymers as drugs, drug and protein conjugates and gene delivery systems: past, present and future opportunities. *J. Drug Targeting* **2006**, *14*, 337−341.
(34) Haag, R.; Kratz, F. Polymer therapeutics: concepts and applications. *Angew. Chem., Int. Ed.* **2006**, *45*, 1198−2015.
(35) Eldon, M. A.; Antonian, L.; Burton, K.; Goodin, R.; Bentley, M. NKTR-102, a novel PEGylated-irinotecan conjugate, demonstrates improved pharmacokinetics with sustained exposure of irinotecan and its active metabolite, poster P-0727, 14th European Cancer Conference (ECCO 14), Barcelona, Spain, Sept 23−27, 2007.
(36) Eldon, M. A.; Hoch, U. Population pharmacokinetics of NKTR-102, a topoisomerase I inhibitor-polymer conjugate in patients with advanced solid tumors, abstract 2598, poster 8E, ASCO 2011, Developmental Therapeutics − Clinical Pharmacology and Immunotherapy, Chicago, IL, June 3−7, 2011.
(37) Sapra, P.; Zhao, H.; Mehlig, M.; Malaby, J.; Kraft, P.; Longley, C.; Greenberger, L. M.; Horak, I. D. Novel delivery of SN38 markedly inhibits tumor growth in xenografts, including a camptothecin-11-refractory model. *Clin. Cancer Res.* **2008**, *14*, 1888−1896.
(38) Kurzrock, R.; Goel, S.; Wheler, J.; Hong, D.; Fu, S.; Rezai, K.; Morgan-Linnell, S. K.; Urien, S.; Mani, S.; Chaudhary, I.; Ghalib, M. H.; Buchbinder, A.; Lokiec, F.; Mulcahy, M. Safety, pharmacokinetics, and activity of EZN-2208, a novel conjugate of polyethylene glycol and SN38, in patients with advanced malignancies. *Cancer* **2012**, *118*, 6144−6151.
(39) Hamaguchi, T.; Doi, T.; Eguchi-Nakajima, T.; Kato, K.; Yamada, Y.; Shimada, Y.; Fuse, N.; Ohtsu, A.; Matsumoto, S.; Takanashi, M.;

Matsumura, Y. Phase I study of NK012, a novel SN-38-incorporating micellar nanoparticle, in adult patients with solid tumors. *Clin. Cancer Res.* **2010**, *16*, 5058−5066.
(40) Hoch, U.; Eldon, M. A. Activity of NKTR-102 in nonclinical models of gastrointestinal cancers, abstract P-0025, ESMO: 12th World Congress on Gastrointestinal Cancer, Barcelona, Spain, June 30−July 3, 2010.
(41) Azim, H. A., Jr.; Awada, A. Clinical development of new formulations of cytotoxics in solid tumors. *Curr. Opin. Oncol.* **2012**, *24*, 325−331.
(42) Kehrer, D. F.; Yamamoto, W.; Verweij, J.; de Jonge, M. J.; de Bruijn, P.; Sparreboom, A. Factors involved in prolongation of the terminal disposition phase of SN-38: Clinical and experimental studies. *Clin. Cancer Res.* **2000**, *6*, 3451−3458.
(43) Combes, O.; Barre, J.; Duche, J. C.; Vernillet, L.; Archimbaud, Y.; Marietta, M. P.; Tillement, J. P.; Urien, S. In vitro binding and partitioning of irinotecan (CPT-11) and its metabolite, SN-38, in human blood. *Invest. New Drugs* **2000**, *18*, 1−5.
(44) Kato, A.; Ueyama, J.; Abe, F.; Hotta, K.; Tsukiyama, I.; Oshima, T.; Kondo, F.; Saito, H.; Hasegawa, T. Panipenem does not alter the pharmacokinetics of the active metabolite of irinotecan SN-38 and inactive metabolite SN-38 glucuronide (SN-38G) in rats. *Anticancer Res.* **2011**, *31*, 2915−2922.
(45) Mathijssen, R. H.; van Alphen, R. J.; Verweij, J.; Loos, W. J.; Nooter, K.; Stoter, G.; Sparreboom, A. Clinical pharmacokinetics and metabolism of irinotecan (CPT-11). *Clin. Cancer Res.* **2001**, *7*, 2182−2194.
(46) Tallman, M. N.; Miles, K. K.; Kessler, F. K.; Nielsen, J. N.; Tian, X.; Ritter, J. K.; Smith, P. C. The contribution of intestinal UDP-glucuronosyltransferases in modulating 7-ethyl-10-hydroxy-camptothecin (SN-38)-induced gastrointestinal toxicity in rats. *J. Pharmacol. Exp. Ther.* **2007**, *320*, 29−37.
(47) Chen, S.; Yueh, M. F.; Bigo, C.; Barbier, O.; Wang, K.; Karin, M.; Nguyen, N.; Tukey, R. H. Intestinal glucuronidation protects against chemotherapy-induced toxicity by irinotecan (CPT-11). *Proc. Natl. Acad. Sci. U.S.A.* **2013**, *110*, 19143−19148.
(48) Nozawa, T.; Minami, H.; Sugiura, S.; Tsuji, A.; Tamai, I. Role of organic anion transporter OATP1B1 (OATP-C) in hepatic uptake of irinotecan and its active metabolite, 7-ethyl-10-hydroxycamptothecin: In vitro evidence and effect of single nucleotide polymorphisms. *Drug Metab. Dispos.* **2005**, *33*, 434−439.
(49) Fujita, K. I.; Sugiura, T.; Okumura, H.; Umeda, S.; Nakamichi, N.; Watanabe, Y.; Suzuki, H.; Sunakawa, Y.; Shimada, K.; Kawara, K.; Sasaki, Y.; Kato, Y. Direct inhibition and down-regulation by uremic plasma components of hepatic uptake transporter for SN-38, an active metabolite of irinotecan, in humans. *Pharm. Res.* **2013**, *31*, 204−215.

Supporting Information

A macromolecular pro-drug that provides the Irinotecan(CPT-11) active metabolite SN-38 with ultra-long half-life, low C_{max} and low glucuronide formation.

Daniel V. Santi, Eric Schneider and Gary W. Ashley

I. General

Reversed-phase HPLC was performed on a Shimadzu UFLC system fitted with a Phenomenex Jupiter 300A 5u C_{18} column thermostatted at 40 ^{o}C and running an ACN/water/0.1% TFA gradient from 20-100% over 10 min. Size exclusion HPLC used a Phenomenex BioSep S-2000 column running 50% ACN/water/0.1% TFA at 1 mL/min. PEG_{40kD}-$(DBCO)_4$ was prepared as described in Ashley *et al* (2013). Azido-linker-alcohols 10A-E were prepared as described (1). Solutions containing SN-38 were quantitated by UV absorbance using $e_{363\ nm}$ = 22,500 at pH 7, and for $e_{414\ nm}$ = 27,500 M^{-1} cm^{-1} at pH 10 (2). NMR spectra were acquired on a JEOL ECX 400 spectrometer, and UV-vis data on a Hewlett Packard 8453 uv-vis spectrometer. SN-38 was from Tecoland Corp. 4-Arm PEG_{40kDa}-$(DBCO)_4$ was prepared as described (3) and PEG_{40kDa}-$(HSE)_4$ was from Jenkem Technology.

II. Syntheses of intermediates

O-[7-Azido-1-(Mod)-heptan-2-yl]-N-(SN-38-CH_2)-N-[4'-(diethylcarbamoyl)phenyl)] carbamates (13) and O-[7-Amino-1-(cyano;-H)-heptan-2-yl]-N-(SN-38-CH_2)-N-[4'-(diethylcarbamoyl)phenyl)]carbamate (15).

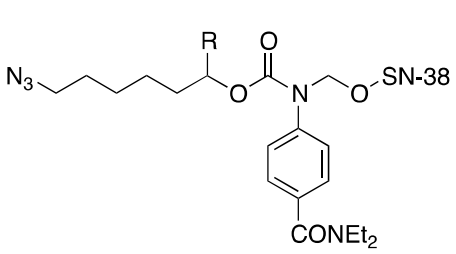

13A-E

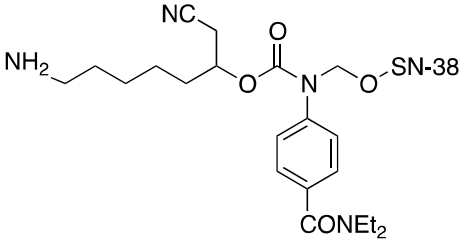

15D,E

N-Aryl carbamates 11A-C,E were prepared as described for 11D using the appropriate anilines.

O-[7-azido-1-(phenylsulfonyl)-2-heptyl]-N-[4'-(diethylcarbamoyl)phenyl)]carbamate (**11A**): colorless glass (500 mg, 97%). ^{1}H-NMR (400 MHz, $CDCl_3$): δ 7.94 (2H, m; H3'), 7.61 (1H, m; Ph-H), 7.54 (2H, m; H2'), 7.33 (4H, m; Ph-H), 6.37 (1H, s; NH), 5.25 (1H,

m; H2), 3.52 (1H, dd, J = 14.9, 7.9 Hz; H1a), 3.5 (4H, br s; NCH_2), 3.37 (1H, dd, J = 14.9, 3.6 Hz; H1b), 3.25 (2H, t, J = 6.9 Hz; H7), 1.74 (2H, m; H2), 1.57 (2H, m; H3), 1.37 (4H, m; H4+H5), 1.18 (6H, br s; CH_2**CH_3**). LC-MS: $[M+H]^+$ = 516.2 (calc. for $C_{25}H_{34}N_5O_5S$ = 516.2).

O-[7-azido-1-(methylsulfonyl)-2-heptyl]-N-[4'-(diethylcarbamoyl)phenyl)]carbamate (**11B**): colorless glass (325 mg, 72%). LC-MS: $[M+H]^+$ = 454.2 (calc. for $C_{20}H_{32}N_5O_5S$ = 454.2).

O-[7-azido-1-(4-morpholinosulfonyl)-2-heptyl]-N-[4'-(diethylcarbamoyl)phenyl)] carbamate (**11C**): colorless glass (425 mg, 81%). LC-MS: $[M+H]^+$ = 525.2 (calc. for $C_{23}H_{37}N_6O_6S$ = 525.2).

O-[6-azidohexyl]-N-[4'-(diethylcarbamoyl)phenyl)]carbamate (**11E**) white crystals from 60/40 EtOAc /hexane (234 mg from 1.00 mmol, 0.65 mmol, 65% yield). ^{1}H-NMR (400 MHz, $CDCl_3$): δ 7.41 (2H, m; H3'), 7.35 (2H, m; H2'), 6.69 (1H, s; NH), 4.18 (2H, t, J = 6.8 Hz; H1), 3.6~3.2 (4H, br; NCH_2), 3.29 (2H, t, J = 6.7 Hz; H6), 1.70 (2H, m; H2), 1.63 (2H, m; H3), 1.44 (4H, m; H4+H5), 1.19 (6H, br; CH_2**CH_3**). LC-MS: $[M+H]^+$ = 362.2 (calc. for $C_{18}H_{28}N_5O_3$ = 362.2).

The following 7-azido-linker-SN-38 analogs 13A-C,E were prepared as described for 13D.

O-[7-Azido-1-(phenylsulfonyl)-2-heptyl]-N-(SN-38-CH_2)-N-[4'-(diethylcarbamoyl)phenyl)]carbamate (**13A)**: 47 mg from 0.1 mmol scale (51%). LC-MS: $[M+H]^+$ = 920.4 (calc. for $C_{48}H_{54}N_7O_{10}S$ = 920.4).

O-[7-Azido-1-(methylsulfonyl)-2-heptyl]-N-(SN-38-CH_2)-N-[4'-(diethylcarbamoyl)phenyl)]carbamate (**13B)**: 41 mg from 0.1 mmol scale (48%). LC-MS: $[M+H]^+$ = 858.4 (calc. for $C_{43}H_{52}N_7O_{10}S$ = 858.3).

0-[7-Azido-1-(4-morpholinosulfonyl)-2-heptyl]-N-(SN-38-CH_2)-N-[4'-(diethylcarbamoyl)phenyl)]carbamate **(13C)**: 110 mg (47%). LC-MS: $[M+H]^+$ = 929.4 (calc. for $C_{46}H_{57}N_8O_{11}S$ = 929.4).

O-[6-azidohexyl] N-(SN-38-CH_2)-N-[4'-(diethylcarbamoyl)phenyl)]carbamate (**13E)**: 107 mg (56%). LC-MS: $[M+H]^+$ = 766.3 (calc. for $C_{41}H_{48}N_7O_8$ = 766.4).

The amino-linker-SN-38 analog 15E was prepared as described for 15D.

O-[6-Amino-2-hexyl] N-(SN-38-CH_2)-N-[4'-(diethylcarbamoyl)phenyl)]carbamate acetate (**16E**). Yield 160 mg (0.186 mmol, 100%) from 186 mmol starting azide. LC-MS: $[M+H]^+$ = 740.3 (calculated for $C_{41}H_{50}N_5O_8$ = 740.4).

III. PEG_{40kDa}-N-aryl-N-(SN-38-CH_2)-N-phenylcarbamates (15 and 16)

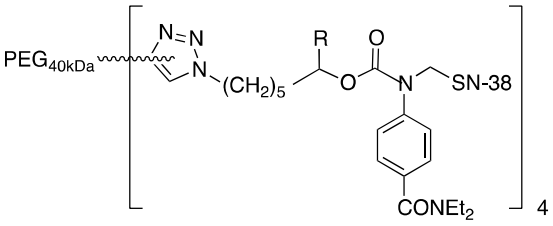

14A-E

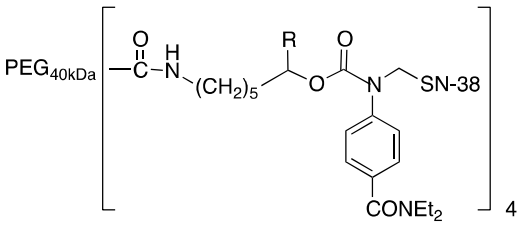

16D,E

The following PEG-SN-38 conjugates 14A-C,E connected with PEG-$(DBCO)_4$ were prepared as described for 14D.

O-[7-PEG-triazole-1-phenylsulfonyl-2-heptyl]-N-(SN-38-CH_2)]-N-[4'-(diethylcarbamoyl)phenyl)]carbamate (**14A**): 95 mg (85%). SN-38/PEG = 3.4. Free SN-38 = 4.8%

O-[7-PEG-triazole-1-methylsulfonyl-2-heptyl]-N-(SN-38-CH_2)]-N-[4'-(diethylcarbamoyl)phenyl)]carbamate (**14B**): 101 mg (90%). SN-38/PEG = 3.9. Free SN-38 = 0.9%

O-[7-PEG-triazole-1-(4-morpholinosulfonyl)-2-heptyl]-N-(SN-38-CH_2)]-N-[4'-(diethylcarbamoyl)phenyl)]carbamate (**14C**): 100 mg (88%). SN-38/PEG = 3.8. Free SN-38 = 0.7%

O-[PEG-triazole-hexyl]-N-(SN-38-CH_2)-N-[4'-(diethylcarbamoyl)phenyl)]carbamate (**14E**): 100 mg (88%). SN-38/PEG = 3.8. Free SN-38 = 0.2%

The PEG-SN-38 conjugate 16E connected by an amide was prepared as described for 16D.

O-[6-PEG-carboxamidohexyl]-N-(SN-38-CH_2)]-N-[4'-(diethylcarbamoyl)phenyl)]carbamate **(16E).** 180 mg on 5 μmol scale (4.0 mmol, 81%). Free SN-38 < 0.2%. SN-38/PEG = 3.9.

IV. Large scale preparation of O-[7-PEG-carboxamido-1-cyano-2-heptyl]-N-[4'-(diethylcarbamoyl)phenyl)]carbamate (16D).

(1)O-[7-azido-1-cyano-2-hexyl]-N-chloromethyl-N-[4'-(diethylcarbamoyl)phenyl)] carbamate (**12D**): A suspension of 7-azido-1-cyano-2-hexyl N-(chloromethyl)-4-(N,N-diethylcarboxamido)-phenylcarbamate **11D** (2.00 g, 5.0 mmol), paraformaldehyde (225 mg, 5.5 mmol, 1.5 Eq), chlorotrimethylsilane (2.5 mL, 20.0 mmol, 4.0 Eq), and 25 mL of anhydrous toluene was placed under N_2 atmosphere in a 50-mL RBF fitted with a magnetic stir bar and closed with a rubber septum cap. The sealed flask was heated in a 50 ^{o}C oil bath for 24 h, at which time a clear yellow solution was obtained. The solution was cooled to ambient temperature and evaporated. The residue was redissolved in 10 mL of dry toluene, filtered, and evaporated to provide the crude N-(chloromethyl)-carbamate as an unstable yellow oil containing residual toluene (2.68 g, 119% of expected). This material was dissolved in 10 mL of anhydrous THF and stored under N_2. Formation of the N-(chloromethyl)carbamate was confirmed by addition of 5

μL of the solution to 1.0 mL of 4 mM N,N-diisopropylethylamine in ethanol, followed by reversed-phase HPLC analysis (Phenomenex Jupiter 300A 4.6x150 mm C_{18}; 1.0 mL/min; gradient from 20-100% CH_3CN/H_2O/0.1% TFA over 10 min). Starting carbamate elutes at 8.42 min and shows λ_{max} 243 nm; product N-(ethoxymethyl)-carbamate elutes at 8.52 min and shows λ_{max} 231 nm; an unknown impurity elutes at 8.04 min and shows λ_{max} 245 nm. Peak integration at 240 nm indicated approximately 89% of the N-(ethoxymethyl)carbamate of **11D**, presumed to represent the purity of **12D**.

^{1}H-NMR (400 MHz, $CDCl_3$): δ 7.39 (4H, m, PhH), 5.54 (1H, d, J = 12 Hz, NCH_aO), 5.48 (1H, d, J = 12 Hz; NCH_bO), 4.99 (1H, m, H2'), 3.51 (4H, br, NCH_2), 3.26 (2H, t, J = 6.8 Hz; H7), 2.79 (1H, m; $H1_a$), 2.63 (1H, m; $H2_a$), 1.85 (1H, m; H3a), 1.73 (1H, m; H3b), 1.60 (2H, m; H4), 1.43 (4H, m; H5+H6), 1.16 (6H, br; NCH_2CH_3).

(2) O-[7-azido-1-cyano-2-heptyl]-N-(SN-38-CH_2)]- N-[4'-(diethylcarbamoyl)phenyl)] carbamate **(13D).** SN-38 (1.00 g, 2.55 mmol) was suspended in 10 mL of anhydrous pyridine, then concentrated to dryness under vacuum (bath temperature 50 °C). This was repeated with 10 mL of anhydrous THF. The resulting pale yellow solid was dissolved in 50 mL of anhydrous THF and 50 mL of anhydrous DMF under N_2 atmosphere, then cooled on ice. A 1.0 M solution of potassium *tert*-butoxide in THF (2.55 mL, 2.55 mmol) was added forming an initial dark green color that changed to a thick orange suspension. After 15 min, a THF solution of the N-(chloromethyl)carbamate **12D** (7.5 mL, 2.8 mmol) was added. After 15 min at 4 °C, the light orange mix was allowed to warm to ambient temperature. After 1 hr, HPLC analysis (5 μL of sample + 1 mL of ACN/TFA) indicated 86/14 product/SN-38. The pale yellow mixture was diluted with 200 mL of EtOAc , washed 2x100 mL of water, 100 mL of sat. aq. NaCl, dried over $MgSO_4$, filtered, and evaporated. Excess DMF was removed by trituration of the oily residue with water, and the residue was dissolved in 50 mL of ACN, filtered, and evaporated to yield 2.96 g of yellow glass. The residue was chromatographed on SiO_2 (80 g) using a step gradient of 200 mL each of hexane, 20%, 40%, 60%, 80%, and 100% acetone in hexane, providing the purified azido-linker-SN-38 (1.66 g, 81%). This material was dissolved in 50 mL of acetone, and 45 mL of 0.1% acetic acid in water was added dropwise with stirring until the mixture became cloudy. Upon stirring, a solid material separated. An additional 5 mL of 0.1% acetic acid in water was then added to complete the precipitation. After stirring for 2 h, the solid was collected by vacuum filtration, washed with water, and dried to provide 1.44 g (1.8 mmol, 70%) of the product as a light yellow powder.

^{1}H-NMR (400 MHz, $CDCl_3$): δ 8.15 (1H, d, J = 9.2 Hz; H12), 7.60 (1H, s; H14), 7.48 (1H, dd, J = 2,9 Hz; H11), 7.40 (4H, m; PhH), 7.25 (1H, d, J = 2; H9), 5.75 (2H, br; NCH_2O), 5.73 (1H, d, J = 16 Hz; H22a), 5.28 (1H, d, J = 16 Hz; H22b), 5.22 (2H, s; H5), 4.99 (1H, m; H2'), 3.84 (1H, s; OH), 3.53 (2H, br; NCH_2), 3.53 (2H, br; NCH_2), 3.17 (2H, t, J = 7 Hz; H7'), 3.12 (2H, q, J = 7 Hz; 7-CH_2), 2.74 (1H, dd, J = 1, 17 Hz; H1'a), 2.54 (1H, dd, J = 5, 17; H1'b), 1.86 (2H, m; H19), 1.6 (1H, m; H3'a), 1.46 (1H, m; H3'b), 1.37 (3H, t, J = 7 Hz; 7-CH_3), 1.25 ~ 1.12 (12 H, m; H4'+H5'+H6'+NCH_2**CH_3**), 1.02 (3H, t, J = 7.3 Hz; H18). LC-MS: $[M+H]^+$ = 805.3 (calc. for $C_{44}H_{51}N_8O_8$ = 805.3).

(3) O-[7-Amino-1-cyano-2-heptyl]-N-(SN-38-CH_2)]- N-[4'-(diethylcarbamoyl)phenyl)] carbamate **(15D).** A 1 M solution of trimethylphosphine in THF (2.9 mL, 2.9 mmol) was added to a solution of the azido-linker-SN-38 **13D** (1.13 g, 1.4 mmol) and acetic acid

(0.19 mL, 3.3 mmol) in 10 mL of THF. Gas was slowly evolved. After stirring for 2 h, water (1.0 mL) was added and the mixture was stirred for an additional 1 h. The residue was partitioned between ether and water. The water phase was washed once with EtOAc, and the resulting clear yellow aqueous phase was evaporated to provide 800 mg of yellow foam. This was dissolved in THF, filtered, and quantitated by UV absorbance to provide a solution containing 1.2 μmol (86%) of product. C_{18} HPLC showed a single peak.

LC-MS: $[M+H]^+$ = 779.3 (expected 779.4).

(4) O-[7-PEG-amide-1-cyano-2-heptyl]-N-(SN-38-CH_2)-N-[4'-(diethylcarbamoyl)phenyl)] carbamate **(16D)**. A mixture of 40 kDa 4-arm tetra-(succinimidyl-carboxylmethyl)-PEG (JenKem Technology; 10.0 g, 1.0 mmol HSC), the amino-linker-SN-38 acetate **15D** (1.2 mmol), and N,N-diisopropylethylamine (0.21 mL, 1.2 mmol) in 75 mL of THF was kept at ambient temperature. Coupling progress was monitored by HPLC, which indicated completion of reaction by 90 minutes. After a total of 2 h, the mixture was filtered into 500 mL of stirred MTBE. The precipitate was collected by vacuum filtration, washed with MTBE, and dried under vacuum to provide the conjugate as a waxy pale yellow solid (10.1 g, 95%). Spectrophotometric analysis of a 2.0 mg sample in 1.0 mL of water indicated 0.170 mM SN-38; based on the calculated 0.175 mM SN-38 expected by weight, indicating a conjugate loading of 96%. C_{18}-HPLC analysis indicated a single major peak (98% of total peak area at 363 nm; 97% at 256 nm), with a minor peak of 0.6 mol% of free SN-38. Treatment in basic solution released all SN-38.

V. Kinetic studies. All kinetic procedures and equations were as described (4).

VI. Pharmacokinetic studies.

In vivo studies: rat. Pharmacokinetic assays in the rat were performed on jugular-cannulated female Sprague Dawley rats (n=3) ~275 g in weight. Dosing solutions were prepared at up to 900 μM conjugate (3.6 mM SN-38) in 10 mM NaOAC, pH 5.0 and filtered through a 0.2 micron syringe filter. IV injections were made at 5 mL/kg body weight. Blood samples (300 μL) were collected at 0, 1, 2, 4, 8, 10, 12, 24, 48, 72, and 120 hours and immediately added to 30 μL of 1M citrate/0.1% Pluronic F68, pH 4.5 (5), and centrifuged at 1500 x g for 10 minutes at 4 °C to give ~150 μL plasma samples which were stored frozen at -80 °C until analysis.

In vivo studies: monkey. Pharmacokinetic studies were performed on adult male St. Kitts African green monkeys (*Chlorocebus sabaeus*) (n=2) ~5.5 kg in weight. Sterile-filtered (0.2 μm) PEG-SN-38 conjugate and CPT-11 dosing solutions were prepared the day of administration at 20 mg/mL (455 μM **16E**, 1.8 mM SN-38 equivalents), 42 mg/mL (955 μM **16D**, 3.8 mM SN-38) and 12.5 mg/mL (42.6 mM CPT-11) in saline. IV injections were made at 0.75 mL/kg **16E**, 1 mL/kg **16D** and 2 mL/kg CPT-11 in the saphaneous vein by controlled infusion over 30 min. Blood samples (2.0) were collected from the femoral vein at the following times: pre-dose, 0.5h, 1, 2, 4, 8, 24, 48, 96, and 168 hours after initiation of infusion. The blood samples were immediately added to 200 μL of 1M citrate/0.1% Pluronic F68, pH 4.5 (5), and centrifuged at 1500 x g for 10 minutes at 4 °C to give ~1 mL plasma samples which were stored frozen at -80 °C until analysis.

Analyses. Plasma samples were thawed on ice was treated with two volumes ACN/0.5% AcOH containing 8 ng/mL camptothecin, and centrifuged at 16,000 x g for 10 min. Samples (100 µL; 25 µL plasma) of the supernatants were analyzed by HPLC on a Phenomenex Jupiter C18 column (5 □.300 Å, 150 mm x 4.6 mm column) at 40 °C using a mobile phase of 100 mM KP_i and 3 mM 1-heptanesulfonic acid adjusted to pH 4.0 with H_3PO_4 (buffer A) and 75% ACN in water (buffer B) (6). Samples were eluted over 19 min at 1.0 mL/min using the gradient: 5% B for 3 min, 20% B for 3 min, 20-40% B over 5 min, 40-100% B over 2 min, 100% B for 3 min, and 5% B for 3 min. RT values were SN-38G 7.1 min, SN-38 12.7 min, CPT-11 13.2 min and PEG-SN-38 14.5 min. Sample elution was monitored with a diode array detector (380 nm) and a fluorescence detector with ex 370 nm and em 470 nm for 9 min followed by em 534 nm for 10 min. SN-38G in these samples could not be quantitated because of co-elution of an interfering substance from processed plasma. LLOQ was 10 nM, and LLOD was 3 nM in plasma samples.

For analysis of SN-38G the precipitated plasma samples were treated with 0.45 vol of 1 N HCl prior to HPLC to convert it to the lactone (RT =4.6 min), and the HPLC column and eluent were exactly as reported (6). Here, the SN-38G was separated from the interfering substance in processed plasma. Concentrations were calculated by comparison of peak areas to appropriate standard curves of samples of PEG-SN-38 conjugate, SN-38 and SN-38G in rat plasma, processed as above.

Pharmacokinetic modeling and parameters.

Concentration vs time data. C vs t data for the PEG-SN-38 and SN-38 were fit to a two-compartment model (**Fig. 2, text**) to determine rate constants k_1, k_{12} and k_{21} using eqs. 1-4 and nonlinear regression analysis (Nelder-Mead downhill simplex); here, αisthetime constant and A amplitude for the conjugate distribution phase, and βisthetime constant and B the amplitude for the conjugate elimination phase. The distribution phases of all conjugates used $t_{1/2,a}$ 4 h, a reasonable composite of conjugates tested and decreased the variables in other equations. Since the steady-state rate for loss of a releasable conjugate, k_{elim} is k_1+k_3 (1), values for k_1 for the DBCO- and amide-linked conjugates were estimated as β(**14A**-**D**) - β(**14E**) and β(**16D**) - β(**16E**), respectively. These values were then used to generate curves for the model of Fig. S1, with the concentration data for free SN-38 being fit to determine values for the remaining parameter k_2, using V_d = 0.18 L/kg (7), and assuming $K_{dist} = V_d/V_c$ to reduce the number of variable parameters.

$$Conj_t = Ae^{-\alpha t} + Be^{-\beta\tau} \quad [1]$$

$$k_{21} = (A*\beta + B*\alpha)/(A + B) \quad [2]$$

$$k_{elim} = \alpha*\beta/k_{21} \quad [3]$$

$$k_{12} = \alpha + \beta - k_{21} - k_{elim} \quad [4]$$

$$A + B = C_{max} = Dose/V_c$$

SI Table 1 shows all pharmacokinetic data obtained in the rat and values calculated thereof.

SI Table 1. Pharmacokinetic parameters for PEG-SN-38 conjugates **14A-E** and **16D,E** and released SN-38 in the rat.

Conjugate	**14E**	**16E**	**14A**	**14B**	**14C**	**14D**	**16D**
R-PEG connector	H-DBCO	H-amide	$PhSO_2CH_2$-DBCO	$MeSO_2CH_2$-DBCO	$O(CH_2)_2NSO_2CH_2$-DBCO	$NCCH_2$-DBCO	$NCCH_2$-amide
Peg-SN-38							
umol SN-38	0.22	0.54	2.3	1.0	3.8	3.1	4.9
C_{max}, uM	86	36	379	116	579	387	623
V_d, L/kg	0.011	0.055	0.025	0.032	0.025	0.029	0.029
$t_{1/2,\alpha}$, h	4	4	4	4	4	4	4
$t_{1/2,\beta}$, h	39	58	9	28	30	35	50
$t_{1/2}$ cleavage ($ln2/k_1$), h	– [b]	–	12	99	138	342	362
k_{12}, h^{-1}	0.075	0.066	0.019	0.061	0.063	0.075	0.086
k_{21}, h^{-1}	0.075	0.099	0.122	0.090	0.087	0.066	0.065
k_{el}, h^{-1}	0.041	0.021	0.109	0.047	0.046	0.052	0.037
r^2	0.9397	0.9500	0.9630	0.9804	0.9099	0.9850	0.9390
$AUC_{0-\infty}$, uM•hr	2132	1768	3632	3076	12440	7588	16664
$C_{0,PEG\text{-}SN\text{-}38}$ [c]	32	19.6	177	51	247	118	199
SN-38							
C_{max}, uM	–	–	1.4	–	0.18	0.18	0.38
$t_{1/2,\beta}$, h	–	–	9	–	34	38	58
$AUC_{0-\infty}$, uM•hr	–	–	13.1	–	6	4.2	10.9
$C_{0,SN\text{-}38}$	–	–	1.27	–	0.154	0.065	0.137
SN-38G	–	–		–			
C_{max}, uM	–	–	0.277	–	0.019	0.017	0.026
$AUC_{0-\infty}$, uM*hr	–	–	2.7	–	0.83	0.45	0.86

[a] Complete pharmacokinetic data and parameters of Fig. 2 of text. [b] Not applicable or not determined, – ; [c] C_o is the concentration at t=0 extrapolated from $t_{1/2}$ β.

SI Table 2 shows data from a preliminary pharmacokinetic study in the African green monkey and values calculated thereof assuming blood compartment is 45 mL/kg. One of the eight animals suffered illness and was omitted from the study results. Certain parameters for SN-38 and SN-38G could not be reliably calculated because later points in the data set were below the LLOQ of 10 nM. Likewise, although the AUC of PEG-conjugates from t=0->∞ could be calculated, small molecules could only be reliably quantitated from 0.5 to 4 hr post infusion, and are listed as such for comparative purposes in SI Table 2. None of the deficiencies cited above materially modify statements and conclusions described in the text.

SI Table 2. Pharmacokinetic parameters for PEG-SN-38 conjugates **16D,E** and CPT-11 in the African green monkey.

Administered drug	**16E**	**16D**			CPT-11		
		16D	SN-38	SN-38G	CPT-11	SN-38	SN-38G
Drug, umol	7.7	21.9			247.1		

$t_{1/2}$,β, hr	78.8	64.7	ND[a]	ND	1.7	ND	2
$t_{1/2}$, cleavage, h		360	NA[a]	NA	NA	NA	NA
$V_{d,ss}$,, L	0.33	0.48	ND	ND	3.7	ND	ND
$AUC_{0.5\text{-}4hr}$, uM•hr			37	8.5	255	5.3	80
$AUC_{0\text{-}t\infty}$, uM•hr	2,802	3,423					
$AUC_{SN\text{-}38G}/_{SN\text{-}38}$	NA			0.23			15

[a] ND=not determined, NA= not applicable.

Determination of *in vivo* cleavage rates. This approach, used to calculate the in vivo cleavage rates of PEG-SN38 conjugates studied here (Fig. 3A,B), was briefly described in ref. (1). The concentration of the PEG-SN-38 cleavable complex at time t is given by eq. 5

$$C_{cleavable}(t) = C_0 \bullet \exp[-(k_1 + k_3)t] \quad [5]$$

Where k_1 is the *in vivo* rate constant for cleavage of the linker, and k_3 the elimination rate of the PEG-conjugate. The concentration of the stable complex is described by eq. 6.

$$C_{stable}(t) = C_0 \bullet \exp[-k_3 t] \quad [6]$$

Thus,

$$\begin{aligned} Ln\{C_{cleavable}(t)/C_{stable}(t)\} &= Ln\{C_{cleavable}(t)\} - Ln\{C_{stable}(t)\} \\ &= Ln\{C_0 \bullet \exp[-(k_1 + k_3)t]\} - Ln\{C_0 \bullet \exp[-k_3 t]\} \\ &= Ln\{C_0\} - (k_1 + k_3)t - Ln\{C_0\} + k_3 t \\ &= -k_1 t \end{aligned} \quad [7]$$

Thus, as in Fig. 3A,B of the text, a plot of $Ln\{C_{cleavable}(t)/C_{stable}(t)\}$ versus time will yield a line of slope of $-k_1$.

SI References

1. Santi DV, Schneider EL, Reid R, Robinson L, & Ashley GW (2012) Predictable and tunable half-life extension of therapeutic agents by controlled chemical release from macromolecular conjugates. *Proceedings of the National Academy of Sciences of the United States of America* 109(16):6211-6216.
2. Nabiev I*, et al.* (1998) Spectroscopic and biochemical characterisation of self-aggregates formed by antitumor drugs of the camptothecin family: their possible role in the unique mode of drug action. *Biochemical pharmacology* 55(8):1163-1174.
3. Ashley GW, Henise J, Reid R, & Santi DV (2013) Hydrogel drug delivery system with predictable and tunable drug release and degradation rates. *Proceedings of the National Academy of Sciences of the United States of America* 110(6):2318-2323.

4. Schneider E, Robinson L, Reid R, Ashley GW, & Santi DV (2014) β-Eliminative releasable linkers adapted for bio-conjugation of macromolecules to phenols. *Bioconjugate Chemistry*.
5. Ranby M, Sundell IB, & Nilsson TK (1989) Blood collection in strong acidic citrate anticoagulant used in a study of dietary influence on basal tPA activity. *Thromb Haemost. 1989 Nov 24;62(3):917-22.* 62(3):917-922.
6. Poujol S*, et al.* (2003) Sensitive HPLC-fluorescence method for irinotecan and four major metabolites in human plasma and saliva: application to pharmacokinetic studies. *Clinical chemistry* 49(11):1900-1908.
7. Kato A*, et al.* (2011) Panipenem does not alter the pharmacokinetics of the active metabolite of irinotecan SN-38 and inactive metabolite SN-38 glucuronide (SN-38G) in rats. *Anticancer research* 31(9):2915-2922.